Die approbierte Originalversion dieser Diplom-/Masterarbeit ist in der Hauptbibliothek der Technischen Universität Wien aufgestellt und zugänglich.

http://www.ub.tuwien.ac.at

The approved original version of this diploma or master thesis is available at the main library of the Vienna University of Technology.

http://www.ub.tuwien.ac.at/eng

TECHNISCHE UNIVERSITÄT WIEN
Vienna University of Technology

DIPLOMARBEIT

Thermal performance analysis of buildings in a hot and humid Climate:

The case of the Affandi Museum in Yogyakarta, Indonesia

unter der Leitung von

Prof. Dr. Ardeshir Mahdavi

E 259/3 Abteilung für Bauphysik und Bauökologie

Institut für Architekturwissenschaften

eingereicht an der

Technischen Universität Wien

Fakultät für Architektur und Raumplanung

von

Tina Tezarek

Matrikelnr. 00828072

Haberlgasse 31/6, 1160 Wien

Wien, Juni 2018

KURZFASSUNG

Das Affandi-Museum in Yogyakarta, Indonesien ist eine in den 1970er Jahren errichtete Gebäudegruppe, in der die Werke des zeitgenössischen Malers Affandi ausgestellt werden. Die hohen Temperaturen und die Luftfeuchtigkeit des tropischen Klimas wirken sich negativ auf den Zustand der Gemälde aus und führen zu einem unbehaglichen Innenraumklima und hohen Kühlbedarf.

Das Institut für Kunstgeschichte, Bauforschung und Denkmalpflege der TU Wien, in Zusammenarbeit mit der Universitas Gadjah Mada in Yogyakarta, hat eine umfassende Bauaufnahme und Zustandsdokumentation mit einem Laserscan-Modell des Museums durchgeführt. Außerdem wird an der Donau Universität Krems eine Strategie zur nachhaltigen Konservierung der Gemälde und Zeichnungen entwickelt.

Im Rahmen dieses Projektes ist es Ziel dieser Arbeit, einen einfachen und umfassenden Workflow zur Generierung eines Gebäudesimulationsmodells aus dem bestehenden Punktwolkenmodell zu erstellen. Dieses Gebäudesimulationsmodell wird verwendet, um das thermische Verhalten des bestehenden Gebäudes zu analysieren und verschiedene Optimierungsoptionen zu untersuchen, um den thermischen Komfort zu verbessern und den Kühlungsbedarf zu reduzieren.

In einem ersten Schritt wird anhand von Messdaten das gegenwärtigen Innen- und Außenraumklima, im Hinblick auf Temperatur und relativer Luftfeuchte, analysiert und mithilfe dieser Daten ein kalibriertes Simulationsmodell erstellt. Da die Messdaten zeigen, dass kein thermischer Komfort gegeben ist, wurden verschiedenen Optimierungsvarianten in der Simulation verglichen. Einerseits wurden passive Maßnahmen untersucht, wie Wärmedämmung, reflektierende Dachoberfläche und Nachtlüftung, andererseits wurden aktive Kühlung und Entfeuchtung getestet. Die Ergebnisse wurden an Hand des thermischen Komforts (ASHRAE Standard 55), Überwärmungsindex und Kühlbedarfs verglichen.

Die Ergebnisse zeigen, dass, obwohl die passiven Kühlungsvariante zum Teil die Innenraumtemperatur deutlich absenken und weniger Überwärmung entsteht, aufgrund der hohen Luftfeuchte kein behagliches Innen Raumklima bereitgestellt werden kann. Nur durch eine Kombination aus passiven und aktivem Maßnahmen kann thermische Behaglichkeit und ein reduzierter Kühlbedarf erreicht werden.

ABSTRACT

The Affandi Museum in Yogyakarta, Indonesia, is a building ensemble constructed in the 1970s, which houses the artwork of contemporary painter Affandi. The high temperatures and the humidity of the tropical climate are causing concerns about the condition of the paintings as well as an uncomfortable indoor climate, which leads to a high cooling demand.

The department of history of art, building archaeology and restoration of TU Vienna in cooperation with the Universitas Gadjah Mada, in Yogyakarta carried out a building survey including a laser scan model of the building site. Additionally, a strategy for the sustainable preservation of all paintings and drawings was developed at Danube University Krems.

The aim of this thesis is to create a simple workflow for the generation of a building simulation model from the existing point cloud model. This building simulation model is then used to analyze the thermal behavior of the existing building and to examine various optimization options to reduce the cooling demand.

In a first step, the onsite measured temperature and relative humidity were used to analyze the current indoor and outdoor climate. Since the measured data showed that temperature and relative humidity are too high to achieve comfortable indoor conditions for staff and visitors, different optimization options were compared through simulation. On the one hand passive measures were tested, such as thermal insulation, white roof, and night ventilation and on the other hand active cooling and dehumidification were analyzed. The results were compared regarding thermal comfort, overheating index, and cooling demand.

Although the passive cooling options significantly reduce the interior temperature and overheating, thermal comfort could not be fully provided due to high humidity levels. Only a combination of passive and active measures were shown to achieve thermal comfort and the reduce cooling demand.

Keywords

Simulation, thermal building performance, museum, tropical climate.

CONTENTS

1 Introduction 1

1.1 Overview 1

1.2 Motivation 2

1.3 Background 3

1.3.1 Overview 3

1.3.2 The Affandi Museum 3

1.3.3 From point cloud to BIM 6

1.3.4 Thermal comfort in hot and humid climate 9

2 Method 11

2.1 Overview 11

2.2 Data acquisition/transfer 11

2.2.1 The Workflow 12

2.2.2 Problems and Drawbacks: 15

2.3 Climate 17

2.3.1 Monitoring 18

2.3.2 Weather file 21

2.4 Building information / Base case 23

2.5 Simulation procedure 27

2.5.1 Simulation Steps 27

2.6 Optimization scenarios 28

2.6.1 Insulation OS1 28

2.6.2 White Roof OS2 28

2.6.3 Ventilation OS3 28

2.6.4 Cooling OS4/OS5 29

2.6.5 Cooling and dehumidification OS6/OS7 29

2.6.6 Active cooling, dehumidification and insulation OS8 30

2.6.7 Active cooling, dehumidification and white roof OS8 30

3 Results 32

3.1 Overview 32
3.2 Thermal comfort 32
3.2.1 Simulation with MEWF:....33
3.2.2 Simulation with GLWF: 38
3.2.3 Simulation with MOWF: 40
3.3 Overheating Index 42
3.3.1 Simulation with MEWF:....43
3.3.2 Simulation BC1:....43
3.3.3 Simulation OS3:....44
3.4 Cooling Load 44
3.4.1 Simulation with MEWF:....45
3.4.2 Simulation BC1:....46
3.4.3 Simulation OS6:....47
3.4.4 Simulation OS9:....48
4 Discussion 49
4.1 Overview 49
4.2 Thermal comfort 49
4.3 Overheating Index 51
4.4 Cooling Load 51
5 Conclusion....53
6 Index....54
6.1 List of Figures....54
6.2 List of Tables....55
6.3 List of Equations....56
7 References....57
8 Appendix 59
A. Psychometric charts....59
B. Weather files....67

1 INTRODUCTION

1.1 Overview

The Affandi Museum in Yogyakarta, Indonesia is a building ensemble which houses the artwork of the contemporary artist Affandi. The high temperatures and humidity of the tropical climate are causing concerns about the condition of the paintings as well as an uncomfortable indoor climate.

The department of history of art, building archaeology and restoration of TU Vienna, in cooperation with the Universitas Gadjah Mada, carried out a building survey which included the creation of a laser scan model of the building site.

Within the framework of this project, the objective of this thesis is to create a simple comprehensive workflow for the generation of a building simulation model from the existing point cloud. This building simulation model will then be used to analyse the thermal performance of the existing building and to explore different optimization options to provide more comfortable indoor conditions and to reduce the cooling demand.

In the first part of this thesis work the motivation will be presented as well as background information regarding recent approaches on the transformation from point cloud to BIM data, as well as thermal comfort in tropical climate.

The second chapter discusses the applied methods to archive the objective of the thesis. First, the necessary steps for transformation of point cloud data to the BIM model are described and documented in detail and problems and drawbacks are outlined. Then, the monitored climate data as well as the generated weather files are discussed. In the next part the parameters of the base case (the existing building) will be explained, followed by the description of the optimization scenarios.

In the third chapter the results of the simulation will be presented starting with the thermal comfort analysis of the different optimization scenarios and followed by the overheating index as well as the comparison of their cooling loads.

The thesis concludes with the discussion of the results and the conclusion.

1.2 Motivation

The buildings sector is one of the largest energy-consumers, accounting for over one-third of final energy consumption globally and thus is responsible for equally important part of CO2 emissions (OECD and IEA, 2013).

According to OECD and International Energy Agency (2013), space heating and cooling, together with water heating, consume nearly 60% of global energy in buildings. It is expected that the demand for space cooling will triple between 2010 and 2050.

Especially in countries with a fast-growing economy as the ASEAN region, consisting of the member states: Brunei, Cambodia, Indonesia, Laos PDR, Malaysia, Myanmar, Philippines, Singapore, Thailand and Vietnam, the energy demand is rapidly rising in recent years. This growth has been accompanied social changes as many people move from traditional homes at the countryside to the city. Urbanization and increased wealth has driven the demand for space cooling and appliances, leading to increasing energy consumption. The share of cooled houses is expected to grow from roughly 10% in 2010 to 60% by 2050.

Space cooling offers thus a large field for improvement strategies to reduce energy consumption and CO2 emissions.

The international energy agency recommends reducing the need for cooling by passive heat rejection perspective, like highly reflective external surfaces, reflective surfaces, low emissivity coating and night time ventilation.

While those OECD recommended strategies have been proven to be effective in hot climate there is little research on to what extend they can improve the thermal comfort in tropical climate.

The objective of this thesis is to carry out thermal performance assessment of the Affandi Museum as a case study to identify the best retrofit strategy to improve thermal comfort and to reduce the cooling demand in hot and humid climate.

1.3 Background

1.3.1 Overview

This chapter provides background information on several topics that are important for this thesis. First, an overview of the research on the Affandi museum will be given, then the state of the art on the data transformation from point-cloud to BIM models will be discussed. In the third part of this chapter the current research on thermal comfort in hot and humid climates will be presented.

1.3.2 The Affandi Museum

The Affandi Museum is located in Yogyakarta in Indonesia and it hosts the artwork of the artist Affandi, an Indonesian expressionist painter. The Museum opened in 1974 and the Artist lived and worked there until his death in 1990. The Museum consists out of several buildings which houses galleries as well as a shop and a restaurant. The area of the Museums ensemble is about 3500m^2. (Figure 1)

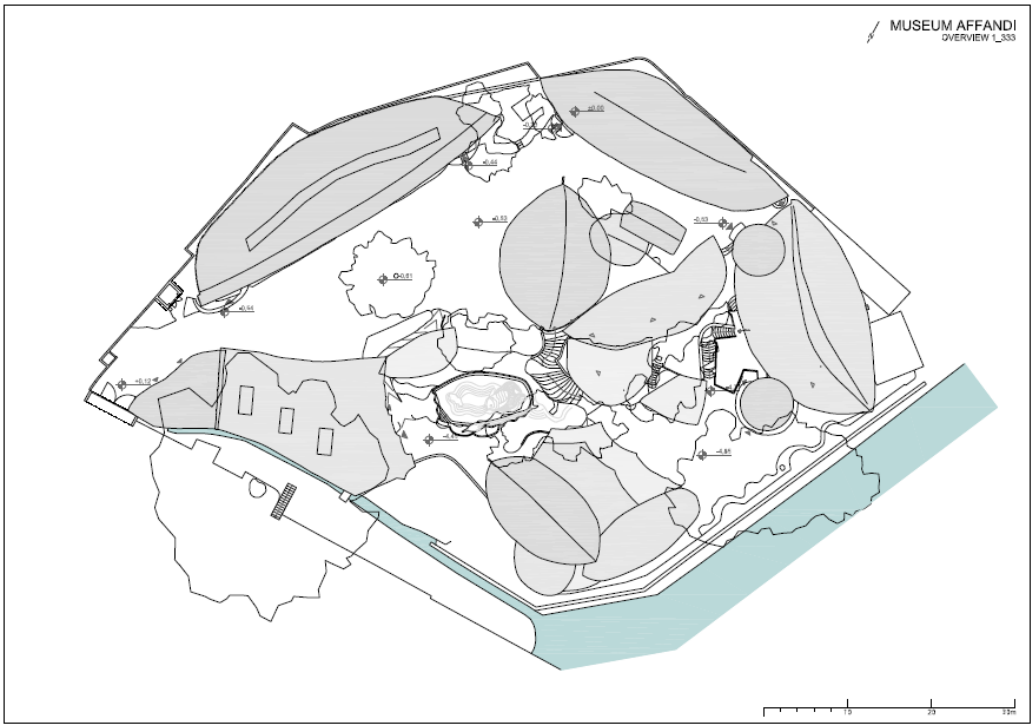

Figure 1 Site plan, Affandi Museum

The architecture of the buildings was inspired by the traditional local Indonesian architecture and was mostly designed by the artist himself. The shape of the banana

leave has been an inspirational element, which is repeated several times in the design of the roofs. (Herbig et al. 2016)

Figure 2 Affandi Museum (source: Ulrike Herbig, 2016)

In 2006 parts of the Museum were destroyed by an earthquake. After that some galleries were reconstructed slightly different and with other materials. (Herbig et al. 2017)

Today, the buildings and the paintings are suffering from the high humidity, as well as the air and water leakage, which lead to mold growth, stress on the artwork and uncomfortable indoor conditions for the visitors and staff. Air conditioning units are installed which, due to extensive operation, might increase the thermal stress on the paintings. The chilled air also might worsen the moisture problem. (Herbig et al. 2016)

The institute of history of art, building archaeology and restoration from the TU Vienna, together with Danube University Krems, European Research Centre for Book and Paper Conservation-Restoration and the Department of Architecture and Planning, Faculty of Engineering, from the University Gadjah Mada in Yogyakarta are working on an interdisciplinary research project about the analysis and conservation of the Affandi Museum. For this project a 3D point cloud model was created. (Figure 3) The acquisition of data was done with a 3D laserscanner VZ-400 from Riegel Laser Measurement Systems, combined with a Nike on D800 DSLR camera. The resulting geometric data set includes also color information and was used for all subsequent activities

Figure 3 Gallery 1, laser scan (source: http://potree.org/demo/tuwien_baugeschichte/examples/museum_affandi.html)

To document further the current state of the building a 'Raumbuch' (room book) was created which documents the damages on the building and describes materials.

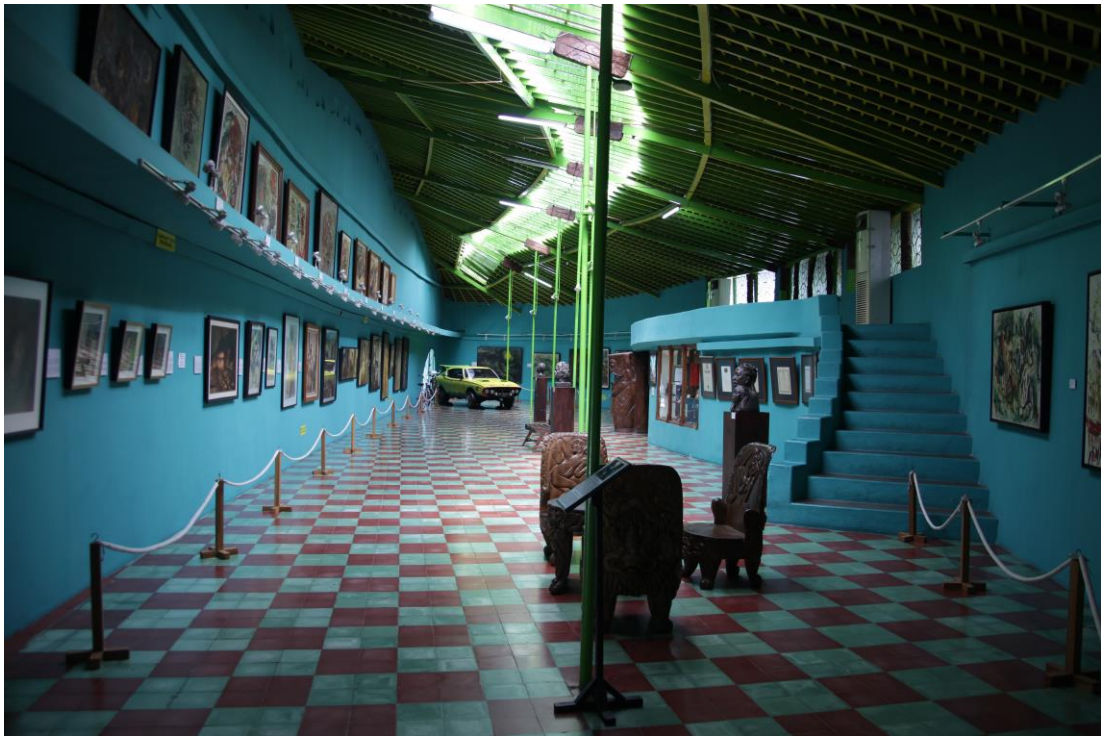

Figure 4 Gallery I (source: Ulrike Herbig, 2016)

For the purpose of this study one gallery (Gallery I) is chosen to conduct the thermal assessment, due to the similarity of the buildings it is assumed that the results are

applicable also to the other buildings of the ensemble. More detailed information on the Gallery 1 can be found in chapter 2 2.4

Due to the variety of issues that concern historic buildings like the Affandi Museum, from documentation of the art work to the indoor climate, there is a strong necessity of integrated approaches.

The Affandi Museum provides a perfect case study for the development of a workflow to combine data from a building survey, architectural research, indoor climate measurements and the documentation of artwork in a challenging environment. The BIM Model provides an environment to store information from different domains.

1.3.3 From point cloud to BIM

Building information modelling (BIM) gained acceptance in architecture, engineering and construction as a tool to store and exchange building related information in a central object-based model, which holds geometric as well as semantic information. This model can later be used to extract information for various purposes. Especially in highly collaborative processes, like restauration or reconstruction work, were the exchange of information between different parties is crucial, the sharing of a centralized model is important. Unlike a traditional CAD model which represents a wall as a set of independent lines, a BIM model represents a wall as a single volumetric object with multiple surfaces, as well as its relationships to other adjacent objects and other properties like material, cost etc. Although BIM has been studied for existing buildings, it is rarely used for modelling existing buildings. (Thomson and Boehm 2015, Dobelis et al. 2016)

This is a consequence of the fact that the 3D data acquisition needed for the BIM model is a long and tedious process, if done manually. Moreover, in historic buildings blueprints are often outdated, inaccurate or simply missing, therefore, laser scanning is a fast way to create accurate 3 D models and walkthroughs. According to Dobelis et al. (2016) laser scanning is the fastest method of 3D data document existing buildings with complex structure in 3D.

One challenge in working with laser scanning is the size of the point cloud, as the laser scanner cannot distinguish between necessary and unnecessary details, like furniture. To further use point cloud for simulation or restructuring work, the 3D model needs to be further simplified. Different tasks require models with different complexity. For example 3D geometry needed for simulation purposes require models with a low complexity (Turner et al. 2015)

According to Tang et al. (2010) the process of creating a BIM model from a point cloud consists of 3 steps:

1. data collection: in which dense point measurements of the facility are collected
2. data processing: in which the resulting point cloud is filtered and misleading points (e. g. from reflections) are removed and the single scans are united in a single coordinate system
3. modelling of the BIM: in which the point cloud is finally transformed in a semantically rich BIM.

According to Dobelis et al. (2016) the manual generation of a BIM model is the fastest and most efficient workflow. This method also minimizes the time for post-work and error fixing from automated model generation.

Tang et al. (2010) suggests that there are two main methods to model a BIM manually. One technique is to fit geometric primitives directly into the point cloud. There are also tools which can do that in a semi-automated fashion. The user has to select some points and an object will be fitted to the selected data. Such tools are based on a region growth algorithm which can extend the contiguous data within a tolerance range. Another technique is to cut the point cloud into horizontal and vertical cross sections and then extrude the geometry. This approach is less computationally intensive. However, the BIM categories have to be chosen manually by the modeler, when the object is created.

The workflow from point cloud to BIM is labor-intensive, subjective and time consuming therefore its automation seems desirable. There is extensive research going on in computer science as well as in geomatics on the automated reconstruction of a BIM model from point cloud data. However, automated creation of BIM models has limited success for existing buildings as they are not rectangular shaped and often contain building elements which are neither horizontal nor vertical

Turner et al. (2015) describes a method in which he first automatically generates a floorplan from the point cloud and then extrudes a 3D model from the 2D plans. This approach is especially useful when a simplified model is needed as it removes all clutter related to furniture. Because of its simplification such models can be used in building simulation applications were the number of elements to represent the building geometry is limited.

Tang et al. (2010) state that in all automated BIM modelling algorithms concepts like “walls are vertical” or “walls are inserted in the ceiling” are encoded in the algorithm

either explicitly, through a set of rules, or implicitly through the design of the algorithm. The problem is that such rules are not universal and are difficult to apply for more complex buildings. This challenge could be overcome in the future with programs that learn from experience.

There are commercial tools which claim to able to transform a laser scan model into a BIM model automatically as an example' imaginit' - a plugin to revit:

"IMAGINiT's Scan to BIM moves beyond simple operations to provide you the ability to interact with point clouds, assisting with automated recognition and placement of architectural elements such as walls, columns and MEP elements such as pipes, ducts, conduit and more" (Imaginit)

The main function of this plug-in is wall fitting, where the user picks three points on a wall from which the software detects with a growing algorithm its extents. However, the tool is only capable of detecting planar walls or arched walls which makes it inadequate for historic buildings were walls often not are in geometric shape.

Other software's for editing point clouds that should be mentioned are 'edgewise', by ClearEdge3D which is able to detect surfaces by finding parts of the point cloud that share coplanar points or 'Kubit' by Faro or 'Poincab', which both provide a tool to aid the manual tracing process.

However, there is no commercial software which can ensure the seamless transfer from laser scan data to a BIM model even if there are tools on the market for exporting point clouds. (Hichri et al. 2013)

Current BIM software and exchange formats assume idealized geometries that rarely exist. Therefore, it is necessary to develop approaches and workflows which are able to transform existing geometry from laser scans into BIM models for further processing.

The automation of the evaluation process of the point cloud has a high development potential, so that in future laser scanning will gain even more importance in the modelling of BIM models. Nevertheless, there is still a great potential for optimization and automation in the construction measurement for BIM with regard to the entire workflow, from the on-site data recording to data processing and data provision. With laser scanning, the main effort lies in data post-processing, so the challenge is to minimize the sometimes very high manual data handling effort through intelligent software processes (e.g., improved geometric structure analysis, derivative semantics). (Thomson and Boehm 2015)

1.3.4 Thermal comfort in hot and humid climate

According to the ASHRAE standard 55 thermal comfort is *'a condition of mind that expresses satisfaction with the thermal environment and is assessed by subjective evaluation'*. This standard is based on the heat balance model of the human body , which assumes that the influencing factors for thermal sensation are: activity or metabolic rate, clothing, air temperature, mean radiant temperature, air movement and moisture content of the air.

One widely used thermal comfort models is the PMV (Predicted Mean Vote)/PPD (Predicted Percentage of Dissatisfied) developed by P.O. Fanger which is based on experimental data from surveys conducted in climate chambers under steady conditions. Those surveys ask about the thermal sensation of the subjects on a seven-point scale from cold (-3) to hot (+3). From this survey he developed an equation to predict the predicted mean vote as well as the predicted percentage of dissatisfied.

The ASHRAE Standard 55 is based on this model to set the requirements (max PPD is 20%) of the indoor conditions. It uses a graphic method to visualize the comfort zone. Therefore, it overlays a psychometric chart to indicate at which condition the thermal comfort is achieved during the summer (0.5 clo) and during winter (1 clo).

Another popular thermal comfort model is the adaptive model which is based on the assumption that occupants control their thermal environment by means of clothing and operable windows etc. This method is generally applied to buildings were no mechanical systems are installed.

Since those comfort models have been developed in mostly cold and dry climate their applicability to hot and humid climate as in Indonesia are controversially discussed.

In tropical climate due to the constantly high humidity, heat loss by evaporation is not possible for the human body and thus the possibility to achieve thermal comfort is severely limited. It is assumed that thermal comfort is perceived differently due to the different outdoor conditions. In this context, Feriadi and Wong (2004) showed in a research about thermal comfort in naturally ventilated houses in Indonesia that PMV predicted warmer thermal perception as compared to what the residents in those actually felt. Another finding was that the residents preferred a cooler temperature (26°C) than the neutral temperature that was chosen (29.2°C). This fact implies that the neutral temperature is affected by the experience of the climate and one's ability to modify it.

Luo et al. (2014) argue, that it might be reasonable to choose a different comfort range for hot and humid climate when considering just naturally ventilated buildings,

however, when considering mechanically ventilated buildings the neutrality temperature decreases also in tropical climate.

Also, De Deara and Bragerb (2002) conducted a thermal comfort evaluation, with 160 sample buildings in various climate zones. The results suggested that occupants of buildings with a HVAC system all over the world adapted to the narrow comfort temperature, while occupants of naturally ventilated buildings prefer a wider range of conditions which are closely linked to the outdoor temperature. Furthermore, they found out that the PMV was far more successful to predict accurately in mechanically ventilated buildings

Traditional Indonesian houses used to be built in lightweight materials like wood - unfortunately modern urban buildings mostly use concrete which stores the heat and makes ventilation strategies less effective. Due to extensive use of HVAC the indoor comfort temperature decreases. The classic comfort adaptive model like ASHRAE 55 is in this climate often not applicable, as it applies just for naturally conditioned spaced and in Indonesia in public buildings air conditioning is used extensively. (Matsumoto et al. 2017)

2 METHOD

2.1 Overview

This chapter describes the methods used to achieve the objective of the thesis. The chapter is split into two parts.

The first part will cover the process of the data transfer from the initial point cloud model to the finished BIM model. The aim of this part is to develop a clear documentation of each step of the data transfer and to establish an easy to use workflow, which will be tested, and drawbacks and problems will be analysed.

The second part will deal with the simulation of various optimization scenarios of the museum itself. First the climatic conditions at the location will be described and the monitored data analysed, then the various optimization options will be explained in detail. And finally, the simulation procedure and software and input data will be outlined.

2.2 Data acquisition/transfer

To create a BIM model, which can be used for the simulation in a further step, different types of input data is needed:

1. Data about the **external environment.** This includes information about the location, climate and Surroundings (e. g. topography, trees…)
2. Data about the **physical building**. This includes information about materials used in the constructions as well as the buildings geometry.
3. Data about the **internal environment**. This includes information about occupancy schedules, devices like HVAC systems lightning etc. and operation hours of the devices.

The information about the building geometry, as well as the topography were derived from the point cloud model, which was constructed by the department of history of art, building archaeology and restoration from the TU Vienna.

Information about the weather file came from a weather file created with the software meteonorm. Data about the materials and constructions were taken from the ‘Raumbuch’ a documentation of the museum created by the department of history of art, building archaeology and restoration from the TU Vienna.

Information about the occupancy schedules and operation hours came from staff working at the museum. (see Table 1)

Table 1 Classification of Input Data

GROUPS	INPUT DATA	TYPE	SOURCE
External environment	Location	Coordinates	'Raumbuch'
	Climate	Weather file	meteonorm
	Surroundings (e. g. topography, trees…)	3D model	Laser scan
Physical building	Geometry	3D model	Laser scan
	Materials	Written documentation	'Raumbuch'
Internal environment	Devices (e. g. HVAC, Lights)	Oral information	Museum staff
	Occupancy	Oral information	Museum staff
	Operation	Oral information	Museum staff

2.2.1 The Workflow

To create the full geometry for a BIM model from a laser scan model three steps are necessary (Figure 5):

1. **Data acquisition**: the laser scanning process. In this case this was already performed by the department of history of art, building archaeology and restoration from the TU Vienna. A 3D laserscanner VZ-400 from Riegel Laser Measurement Systems was used.
2. **Data processing**: this step requires a dedicated laser scan post processing software. First the points need to be filtered and misleading points must to be removed and the single scans have to be united in a single coordinate system. This was done in the software Riscan, a dedicated software from the laser scanner manufacturer Riegel. By exporting Riscan produces a file with the data format .laz. This format is a public file format for the interchange of 3-dimensional point cloud data between users.

   Modelling of the BIM: in this step the point cloud will be transformed in a BIM model with a dedicated software. The modelling software Autodesk revit 2016 was chosen, as to the authors knowledge, it is the software, on which

most of the tested point cloud geometry modelling plugins rely on. However, Autodesk revit is not able to import the point cloud directly from riscan due to format incompatibility issues. Therefore, first the point cloud data needs to be imported into recap another software product from autodesk. Recap is able to transform the riscan format .laz into .rcp, which can be imported in revit. The point cloud was cut horizontally and the geometry was extruded. In this step the information from the ‘Raumbuch’ about constructions was added.

3. **Simulation of the 3D model**: in this step the BIM model was exported via .gbXML to Energy Plus a simulation software. Then the information about climate was added by a weather file created by a dedicated software meteonorm. Also, the information about schedules and devices were added in this step manually.

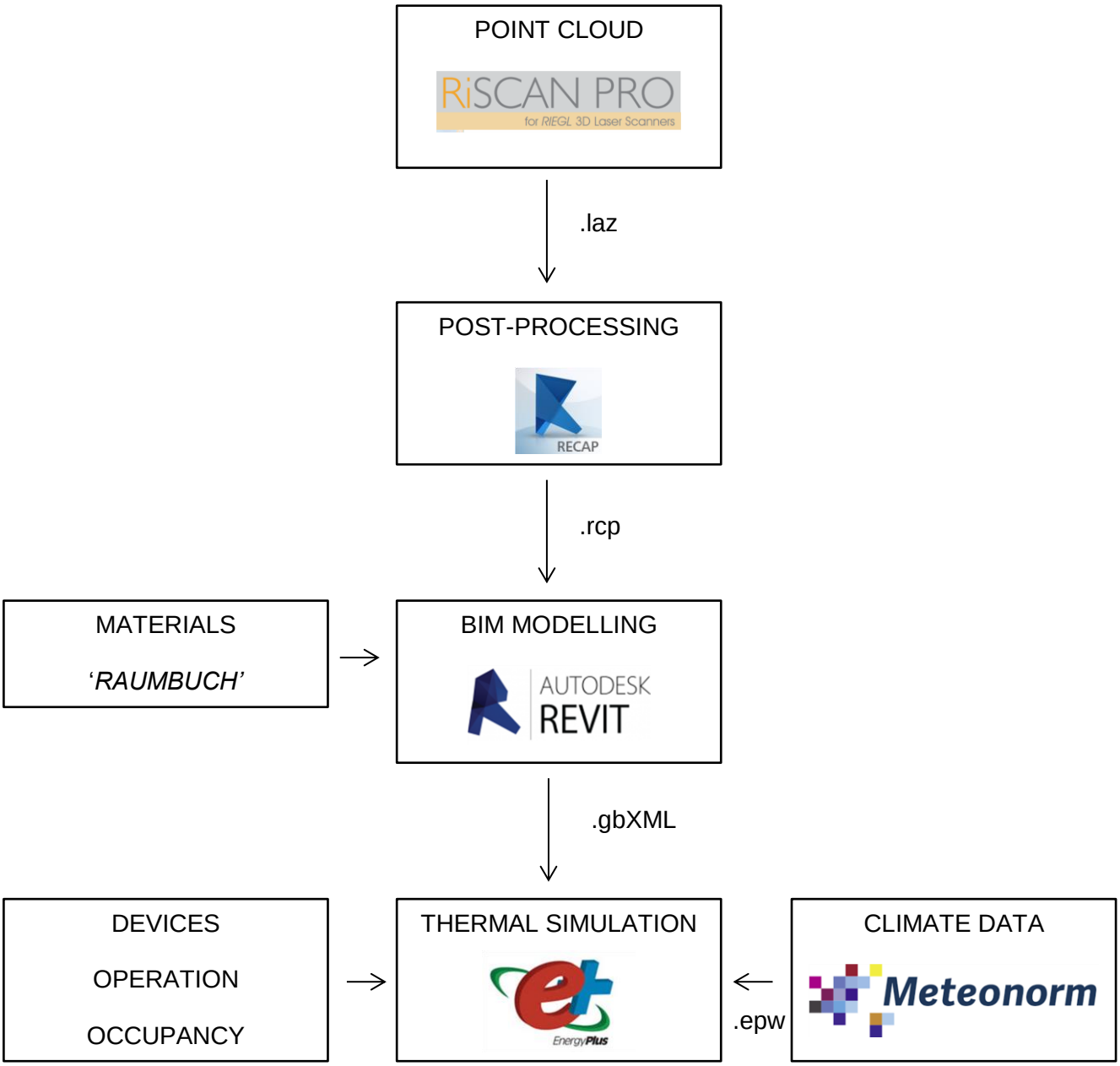

Figure 5 Workflow

2.2.2 Problems and Drawbacks:

There are several disadvantages and limits to this workflow.

1. It is necessary to know lots of software application, which are partly expensive commercial software.
2. The workflow is time consuming and labor-intensive, since the complex geometry of the building makes it impossible to use any automated approaches.
3. The manual tracing process from the point cloud in the BIM modelling program makes the process to some extend subjective to the modeller. (Figure 6)
4. The process of importing and exporting leads to a loss of geometry and information due to incapability of the different software types. (Figure 7, Figure 8)
5. Previous knowledge about the building is still necessary since it is sometimes impossible to recognize objects in the point cloud, for example changes in material on the same surface or to distinguish between furniture and building structure.

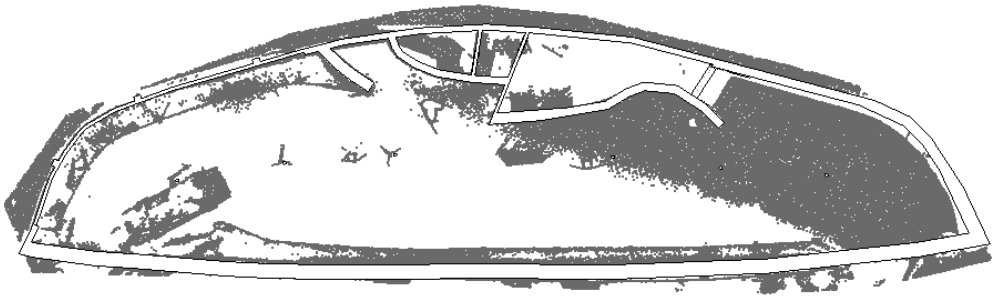

Figure 6 Revit 2016, floor plan in point cloud

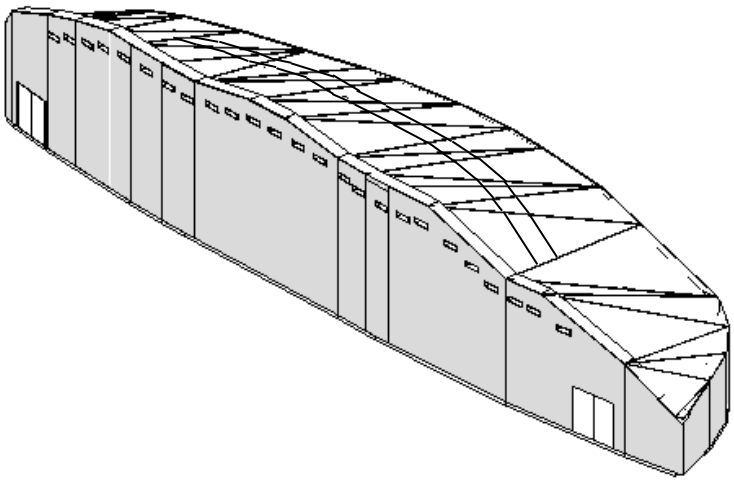

Figure 7: Revit 2016, BIM geometry model, before exporting

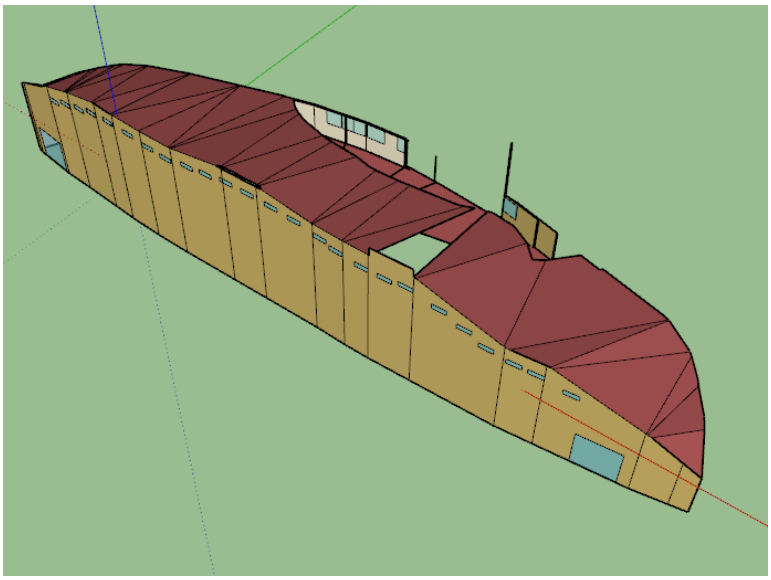

Figure 8 Open Studio, geometry model, after importing via gbXML

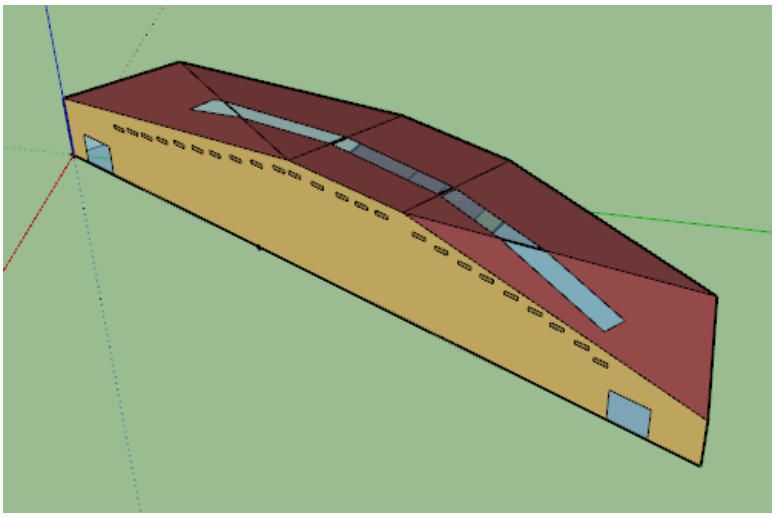

Figure 9 Open Studio, final geometry model

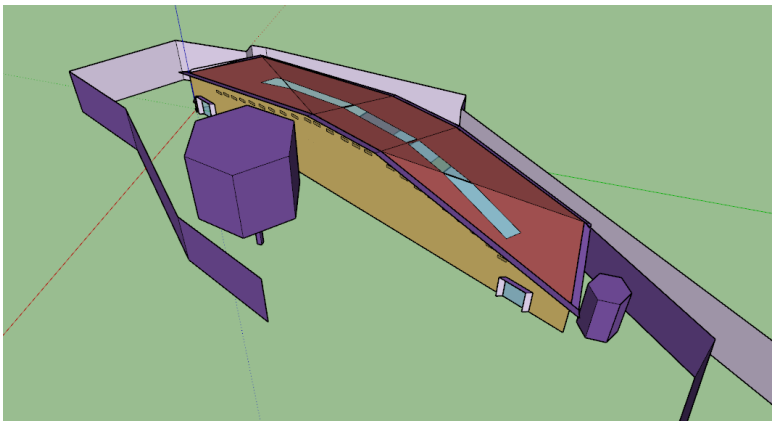

Figure 10 Open Studio, final geometry model with shading

2.3 Climate

Yogyakarta in Indonesia is located in 7° 48′ 5″ S, 110° 21′ 52″ O in the tropics. The climate is generally hot and humid with very little variation throughout the year. (Figure 11, Figure 12). There are no seasons, temperature and humidity are consistently high with little variation between night and day. According to the Koeppen-Geiger climate zones the location is classified as ‘Am’ which means tropical monsoon climate (Figure 13).

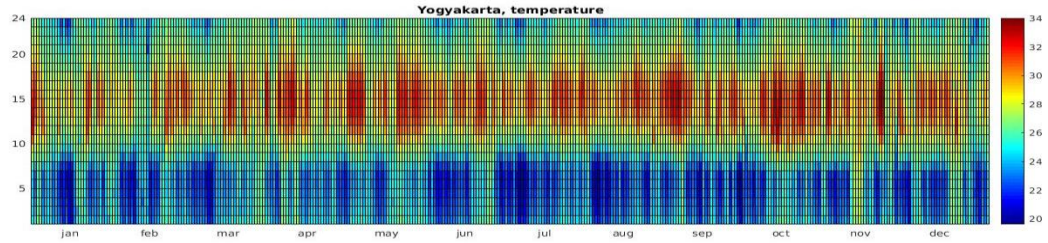

Figure 11 Temperature range in Yogyakarta, meteonorm weather file,

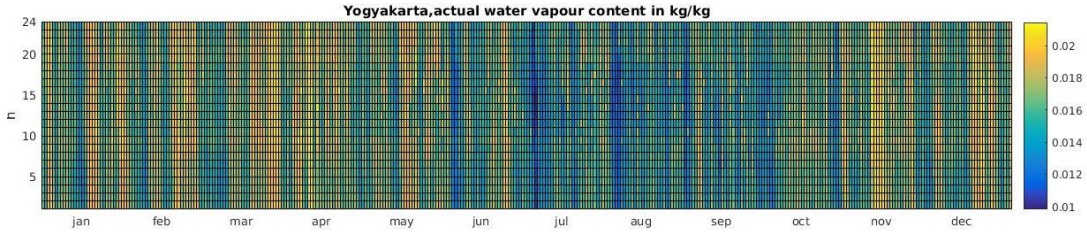

Figure 12 Absolute humidity range in Yogyakarta, meteonorm weather file

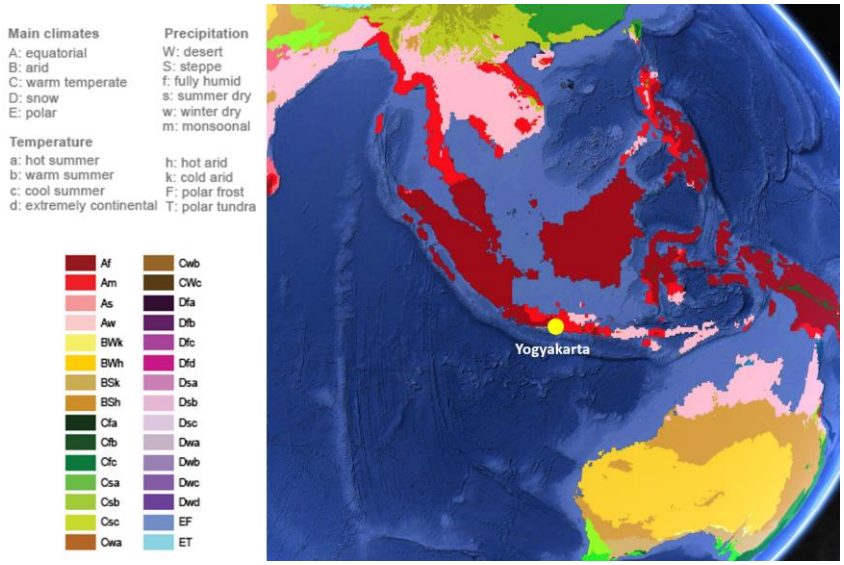

Figure 13 Koeppen Geiger map (source: http://koeppen-geiger.vu-wien.ac.at)

There is only short-term monitored data available of the location. The monitored indoor and outdoor climate will be described in 2.3.1. Since there was no long term monitored weather data available from the location a weather file was generated and will be described in 2.3.2

2.3.1 Monitoring

For the climate monitoring HOBO U12-012 data loggers were used. The sensor measures temperature (-20° to 70°C) with an accuracy of ± 0.35°C and the relative humidity (5% to 95%) with an accuracy of ± 2.5% as well as the light intensity. The measurements were taken in 10 minutes intervals. Several sensors were positioned

inside the galleries and one outside. (Figure 14). Three sensors C, D and E were positioned in gallery 1 (Figure 19). The climate was monitored from 17. 12. 2016 until the 4.1.2016. The psychometric chart shows that the temperature is out of the comfort zone the entire time. (Figure 18)

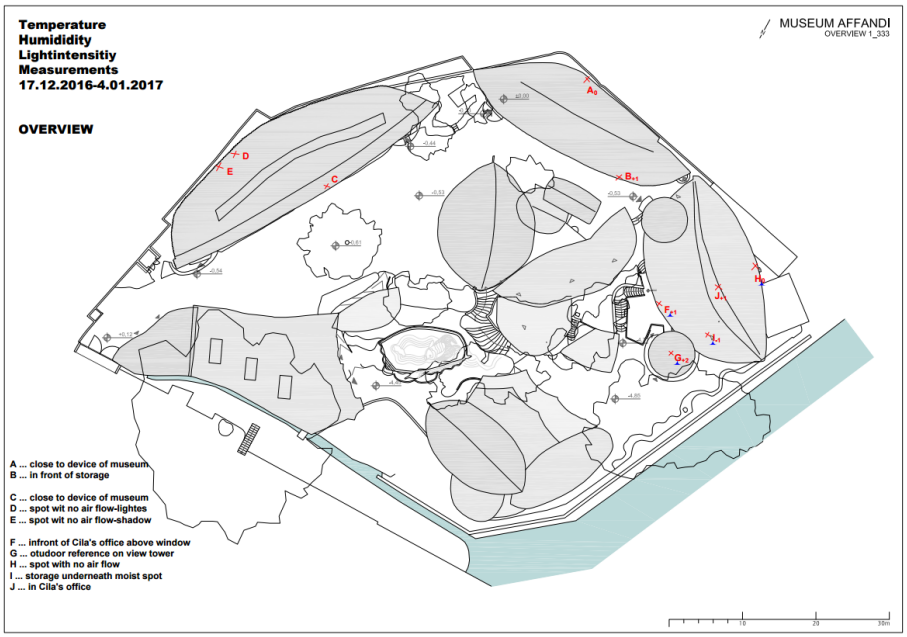

Figure 14 Sensor location in the Affandi museum

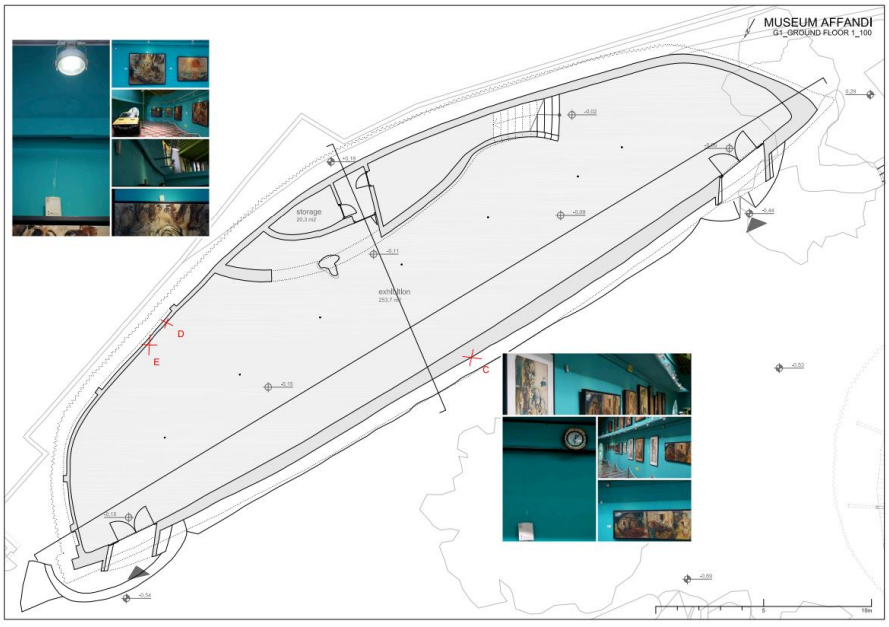

Figure 15 Sensor Location Gallery 1

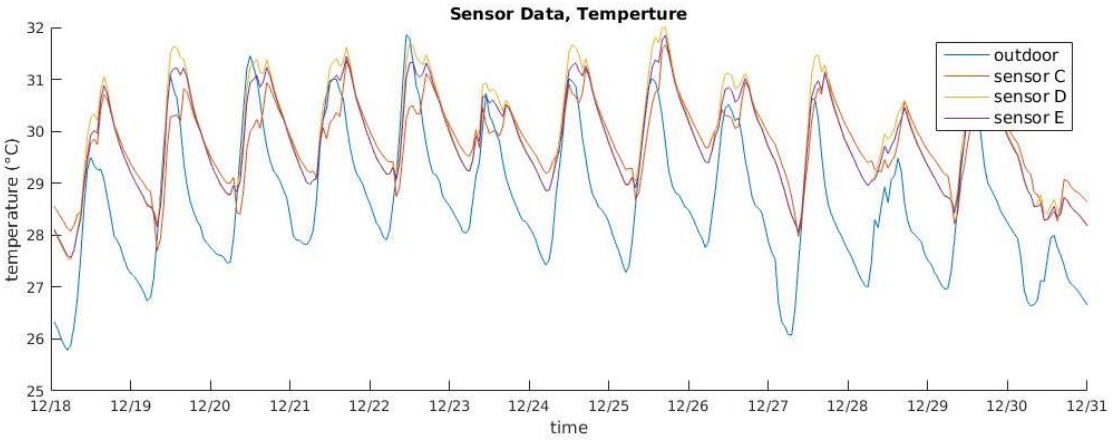

Figure 16 Sensor data, temperature

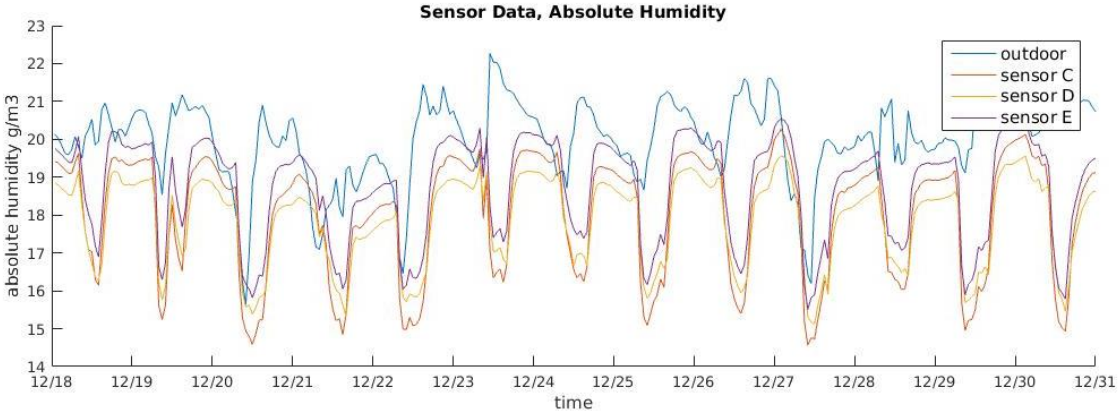

Figure 17 Sensor data, absolute humidity

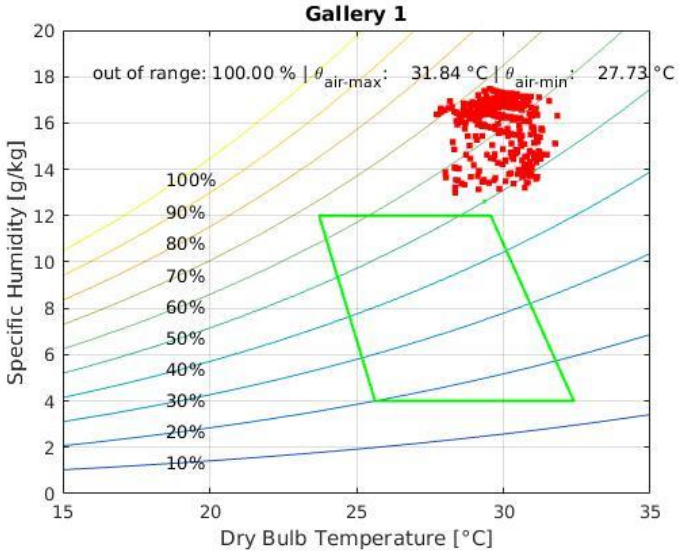

Figure 18 Psychometric Chart, ASHRAE 55, Gallery 1

2.3.2 Weather file

To conduct a simulation that produces meaningful results, weather data for an entire year was needed. Since the available measured data was available for a too short period of time, different weather files were created.

Meteonorm weather file MEWF:
No weather file is available for the location Yogyakarta; therefore an interpolated weather file was created with meteonorm version 7.

The created weather file was compared to the actual measured data. The measured data was 4 °C above the weather file temperature during night-time and 2.5 °C above the weather file temperature during the day (Figure 20).

Since the variation in humidity and temperature over the months is rather small it was assumed that the difference would be the same over the whole year. (Table 2) Therefore, the simulation was conducted with two other weather files. Due to the significant discrepancy between measured data and weather file two other weather files were created to investigate on the influence of the used weather data on the simulation.

Global warming weather file GLWF:
The second weather file was generated with meteonorm assuming a global warming scenario B1 (low, global 2°C warming until 2100). This gives higher temperature and therefore the graph is closer to the actual measured temperature.

Modified weather file MOWF:
The third weather file is a modified version of the original meteonorm weather file. First, mean hourly temperature distribution for a reference day was calculated for the monitored temperature and for the weather file for the period of monitoring. Then, the obtained hourly temperature for the measured data was divided by the hourly temperature from the weather file (Figure 20). Finally, the temperature of the weather file was multiplied by this factor and a new shifted temperature curve was obtained. (equation 1). The same procedure was applied to the absolute humidity.

$$\theta_s = \theta_w * \frac{\theta_{av,h,m}}{\theta_{av,h,w}} \qquad (1)$$

θ_s $modified\ temperature$ ℃

θ_w $weatherfile\ temperature$ ℃

$\theta_{av,h,w}$ $weather\ file\ meateonorm, daily\ average\ for\ one\ hour$ ℃

$\theta_{av,h,m}$ $monitored\ data, daily\ average\ for\ one\ hour$ ℃

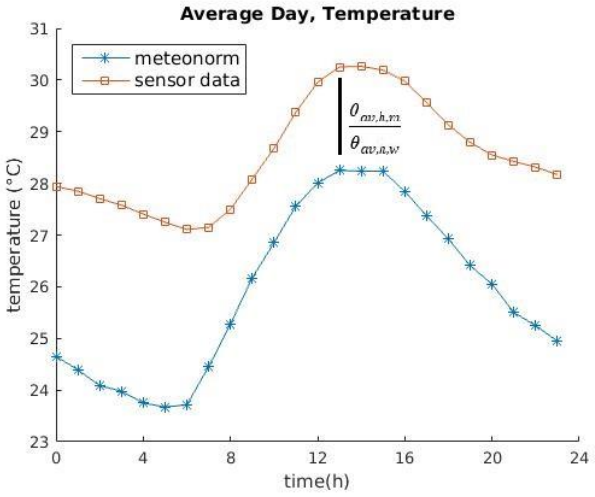

Figure 20 Mean hourly temperature distribution for a reference day

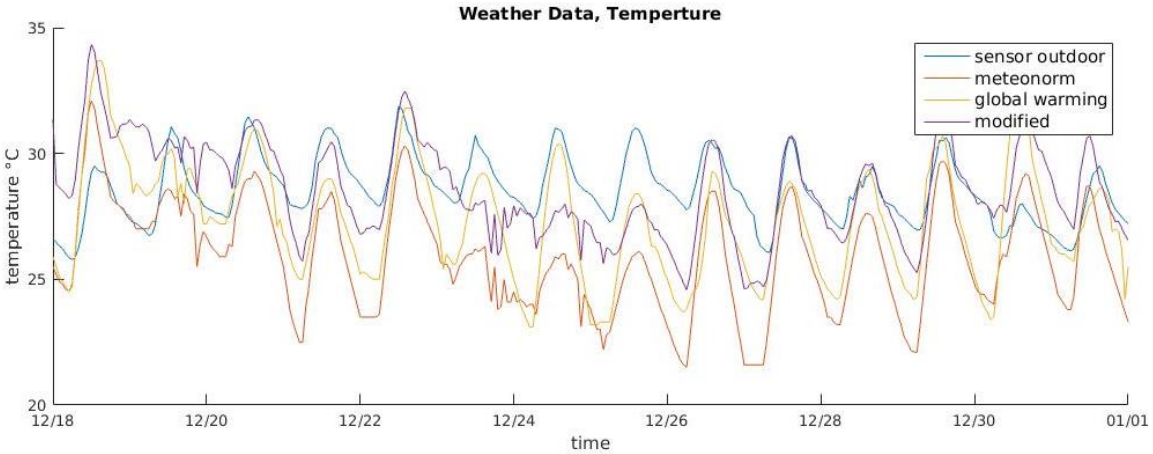

Figure 21 Comparison measured data and weather files

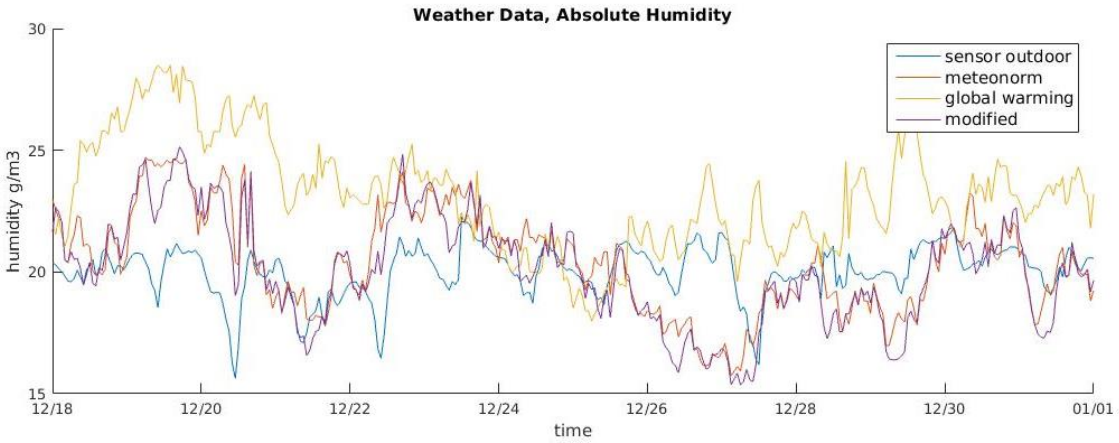

Figure 22 Comparison measured data and weather files

Since only data for humidity and temperature were available, the remaining data like irradiation wind speed and direction remained the same as in the original meteonorm weather file.

Table 2 Comparison weather files, mean monthly temperature °C

Weather files	**Jan**	**Feb**	**Mar**	**Apr**	**May**	**Jun**	**Jul**	**Aug**	**Sep**	**Oct**	**Nov**	**Dec**
MEWF	26	25	26	26	27	26	26	26	26	27	26	26
GLWF	27	27	27	27	28	27	26	27	27	28	27	27
MOWF	28	28	28	28	29	28	28	28	28	29	29	29

2.4 Building information / Base case

The gallery 1 is a building within the building complex of the Affandi Museum.

Some basic information can be found in Table 3.

Table 3 Basic information, Gallery 1

Total floor area [m²]	253.7
Room height [m]	2.83-7.14
Room function	exhibition
Gross wall area [m²]	422.53
Window area [m²]	21.08
Glazing ratio [%]	4.99

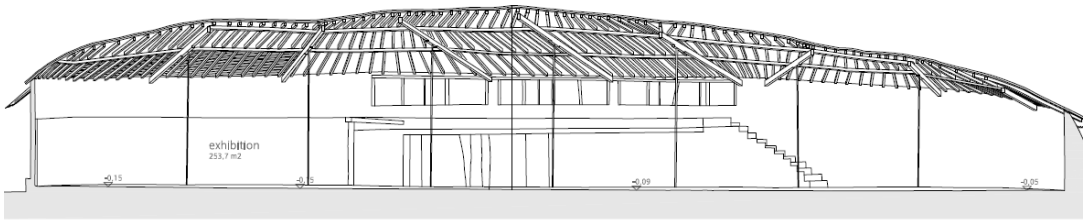

Figure 23 Cross section, Gallery I

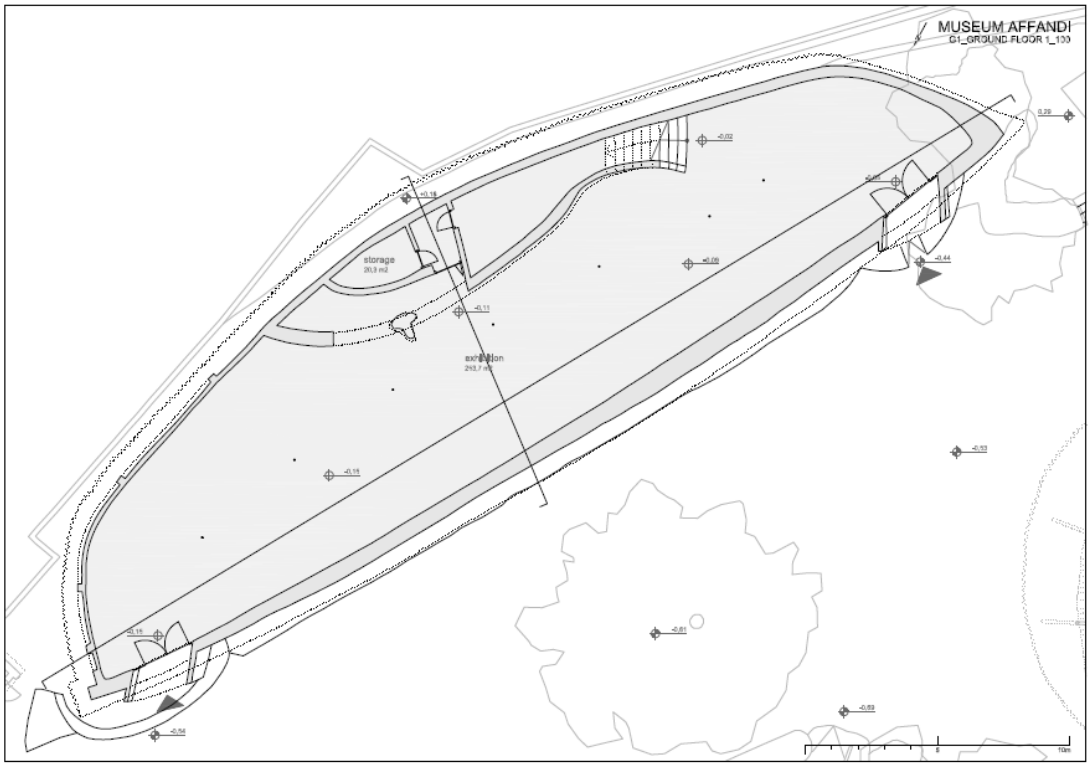

Figure 24 Ground floor, Gallery I

The Gallery consist out of a ground floor and a one story high podium in front of the west wall, housing a storage room. In this space a series of oil paintings as well as the painter Affandi's car are displayed. There are two transparent doors and non-openable windows on the north-west facade and one skylight made of synthetic transparent material. The skylight is covered with a semi-transparent fabric from outside (Figure 25). Beneath the roof used to be a series of openings which have been closed after the earthquake (Figure 26). The walls have a varying thickness and are made of concrete pillars filled with brick masonry, plastered inside and out. Additionally, there is a drywall construction which is used for light installation. The original roof structure was made of wooden beams covered with wooden shingles, as it is used in traditional Indonesian architecture, but since the roof has a very small inclination the water couldn't run off which leaded to water leakage and as a consequence the roof was covered with bitumen shingles.

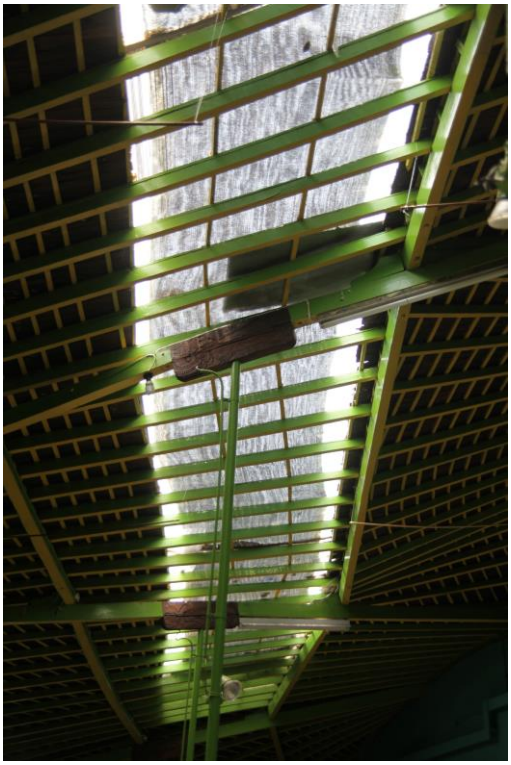

Figure 25 Gallery I, Skylight (source: Ulrike Herbig, 2016)

Figure 26 Gallery I, closed window (source: Ulrike Herbig, 2016)

The materials used for the simulation of the base case are listed in Table *4* and Table *5*.

Table 4 Characteristics of opaque constructions of the building envelope

name	materials	Thickness [mm]	U-Value [W/m²K]
Brick wall	Plaster Brick Plaster Air space Gypsum Board	600 450 250 150	0.856 1.000 1.290 1.509
Roof	Bitumen Wood	50	3.145
Floor	Tiles Concrete	750	2.44

Table 5 Characteristics of transparent constructions of the building envelope

name	Materials	Thickness [mm]	Thermal-, solar-, and visible absorptance
Door, Windows	Acrylic sheet	6	0.9 0.7 0.7

The museum is open for the public daily from 09.00 a.m. up to 04.00 p.m. It is closed for visitors on Sunday, the first Monday in every month and national holidays. This is also the period in which equipment is operating like HVAC systems or lights.

The website of the Affandi museum gives information about the number of visitors every year. The most recent data is from 2010 when 9742 people visited the museum. Considering the opening days, this gives approximately 30 persons per day.

For the activity level it was assumed that people are 'standing relaxed' which corresponds according to 2005 ASHRAE Handbook of Fundamentals a value of 70 W/m^2 (1.2 met).

The hourly air change rate was assumed to be constantly 0.3 h^{-1}.

To make the base case scenario comparable to the passive optimization strategies two base cases were created one with a HVAC system (BC1) and one without (BC2).

2.5 Simulation procedure

The thermal simulation was conducted in 'Energy Plus' version 8.7. 'Energy Plus' is an open source application, supported by the Department of Energy of the USA, which simulates dynamically a buildings thermal performance and the performance of its systems.

2.5.1 Simulation Steps

1. The geometry was imported into Sketchup with the Open Studio plugin as described in 2.2.
2. Thermal zones were assigned. In this case the exhibition space and the small storage room were divided into two separate thermal zones and redrawn were the conversion of the format had failed.
3. The geometry was imported to Energy Plus.
4. The material properties were assigned as well as operational scenarios as internal gains.
5. The model was calibrated with the sensor data from 18.12.2016-31.12.2016.
6. The weather file was assigned
7. The scenario was simulated over a whole year with hourly values for indoor temperature and humidity as well as cooling load.

2.6 Optimization scenarios

Considering the wide range of retrofitting possibilities, for this study nine scenarios were chosen based on economic and technical feasibility. For passive cooling, the strategies were selected from the recommendations of the OECD and International Energy Agency (2013) (OS1-OS3), and four active cooling and dehumidification methods with different setpoints (OS4-OS7). Lastly there are also two options where passive and active cooling strategies are combined. The different scenarios are summarized in Table *6*.

2.6.1 Insulation OS1

Pak et al. (2013) showed in a study the impact of thermal insulation in hot and humid climate. They demonstrated that in a test cell equipped with 50 mm of EPS the thermal comfort could be improved. For the simulation scenario OS1 a thermal insulation of the material EPS with a thickness of 25 cm and a conductivity of 0.036 W/mK was added to all walls of the thermal envelope.

2.6.2 White Roof OS2

White or reflective roof is a design strategy that aims to reduce the effect of heat gain on building roofs by solar radiation.

Urban, B., Roth, K (2010) state that the surface temperature of a dark roof on a hot and sunny day, the temperature of normal dark roofs can be decreased from 66 °C down to 28 °C just by changing the colour.

For the simulation case OS2 it was assumed that the colour of the roof is white with a solar absorptance, visible absorptance of 0.2.

2.6.3 Ventilation OS3

Liping and Hien (2007) analysed natural ventilated houses in Singapore, where the climate is also considered as hot and humid. They showed that that full-day ventilation can improve the thermal comfort in tropical climates.

For this scenario it was assumed that the former openings beneath the roof would be open again during the night-time. Therefore, the air change rate was set to 1 h^{-1} during the day and 3 h^{-1} during the night. The night period was from 12 p.m. until 7 a.m. which is the coolest period of the day according to the daily temperature curve (Figure 27).

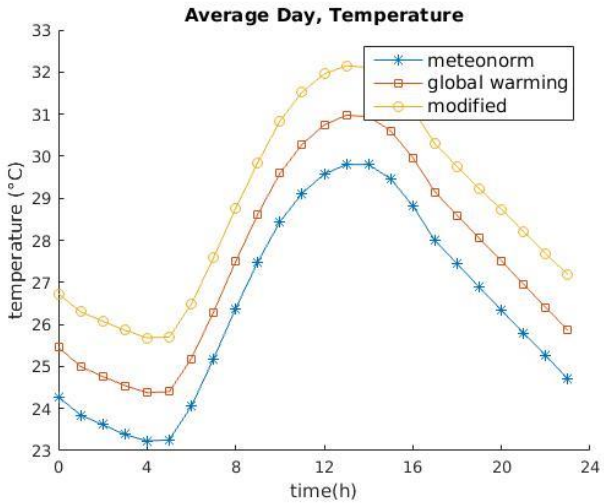

Figure 27 Weather files, mean hourly temperature distribution for a reference day

2.6.4 Cooling OS4/OS5

Besides the passive cooling strategies also active cooling scenarios were simulated. For the cooling scenario the ideal loads air system object was used. This object provides a model for an ideal HVAC system, which supplies cooling or heating air to a zone in sufficient quantity to meet the zone load.

Two different cooling scenarios were modelled. The first one OS5 has a constant setpoint at 25 °C which is the maximum setpoint temperature for museums recommended by ASHRAE (2015).

For the second scenario OS6 it was decided to increase the setpoint temperature to 27°C during the non-operating hours to save energy.

2.6.5 Cooling and dehumidification OS6/OS7

In this scenario also, the ideal loads air system object was used. For the scenario OS6 the system was not only set to a constant cooling setpoint of 25°C but also to a constant dehumidification setpoint of 60% relative humidity, which is also the maximum relative humidity recommended by ASRAE (2015). In the second scenario, OS7, similar to OS5 the cooling setpoint was increased during the non-operational hours.

2.6.6 Active cooling, dehumidification and insulation OS8

This scenario assumes the same parameters as scenario OS1, but active cooling and dehumidification was added as describes in OS7.

2.6.7 Active cooling, dehumidification and white roof OS8

This scenario assumes the same parameters as scenario OS2, but active cooling and dehumidification was added as describes in OS7.

Table 6 Optimization options

code	scenarios	*construction*	*solar absorptance, visible absorptance*	*Air change rate [1/h]*	*HVAC*
BC1	Base case	Construction see Table 4	0.7 0.7	0.3	ideal loads air system setpoint temperature 30°C during operating hours
BC2	Base case No HVAC	Construction see Table 4	0.7 0.7	0.3	no HVAC
OS1	Insulation	Construction see Table 4 + 25cm eps insulation added to wall and roof	0.7 0.7	0.3	no HVAC
OS2	White Roof	Construction see Table 4	0.2 0.2	0.3	no HVAC
OS3	Ventilation	Construction see Table 4	0.7 0.7	1.0 by day 3.0 by night	no HVAC
OS4	Cooling Constant Setpoint	Construction see Table 4	0.7 0.7	0.3	ideal loads air system setpoint temperature 25°C
OS5	Cooling Varying Setpoint	Construction see Table 4	0.7 0.7	0.3	ideal loads air system setpoint temperature operating hours 25°C otherwise 27°C
OS6	Cooling Constant Setpoint Dehumidification	Construction see Table 4	0.7 0.7	0.3	ideal loads air system setpoint temperature 25°C dehumidification setpoint 60%
OS7	Cooling Varying Setpoint Dehumidification	Construction see Table 4	0.7 0.7	0.3	ideal loads air system setpoint temperature operating hours 25°C, otherwise 27°C dehumidification setpoint 60%
OS8	Insulation + Cooling Varying Setpoint Dehumidification	Construction see Table 4 + 25cm eps insulation added to wall and roof	0.7 0.7	0.3	ideal loads air system setpoint temperature operating hours 25°C, otherwise 27°C dehumidification setpoint 60%
OS9	white Roof + Cooling Varying Setpoint Dehumidification	Construction see Table 4	0.2 0.2	0.3	ideal loads air system setpoint temperature operating hours 25°C otherwise 27°C dehumidification setpoint 60%

3 RESULTS

3.1 Overview

This chapter shows the results of the simulation runs. In the first part 3.2 the most significant results of the optimization strategies will be presented in psychometric charts. The complete set of results can be found in the 8 Appendix. Then, in chapter 3.3 the bar graphs of the overheating index of the passive cooling strategies will be shown. In the last part 3.3 the annual cooling loads, as well as the peak cooling loads of the active cooling scenarios will be shown. Each chapter will be divided into 3 parts. Every part shows the simulation results, run with a different weather file.

3.2 Thermal comfort

For the evaluation of the thermal comfort of the passive cooling strategies the Ashrae standard 55 adaptive model was used. For simplicity and lack of information the mean radiant temperature was assumed to be the same as the mean air temperature.

For the evaluation of the active cooling strategies the Ashrae standard 55-2004, using PMV was applied. In this case the thermal comfort is based on dry bulb temperature, clothing level (clo), metabolic activity (met), air velocity, humidity and mean radiant temperature. The zone in which most people are comfortable is calculated using the PMV (predicted mean vote) model. The clothing level was assumed to be 0.5 clo (typical summer clothing) all year around since there is hardly any difference between the seasons. The activity level was set to 1.2 met which corresponds to standing activity. The air velocity was assumed to be between 0.2 and 1,5 m/s. The mean radiant temperature was assumed to be the same as the mean air temperature. The comfort zone was chosen in order to satisfy 90% of the people.

3.2.1 Simulation with MEWF:

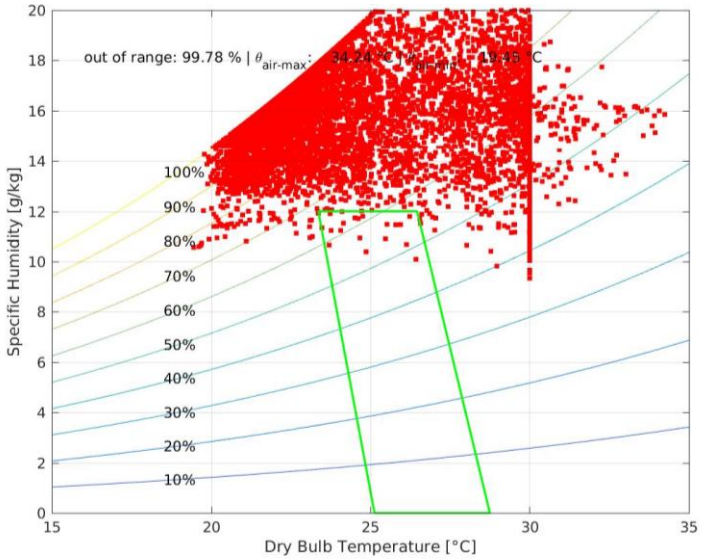

Figure 28 Psychometric chart, Ashrae standard 55, MEWF, BC1

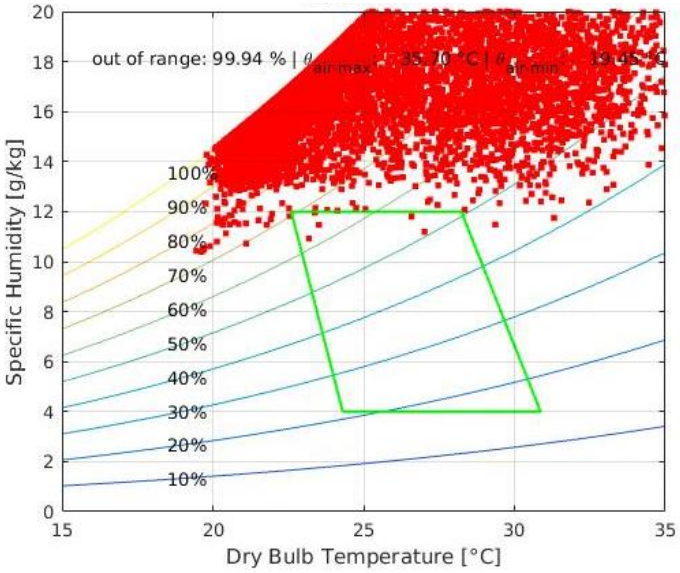

Figure 29 Psychometric chart, Ashrae 55 adaptive comfort, MEWF, BC2

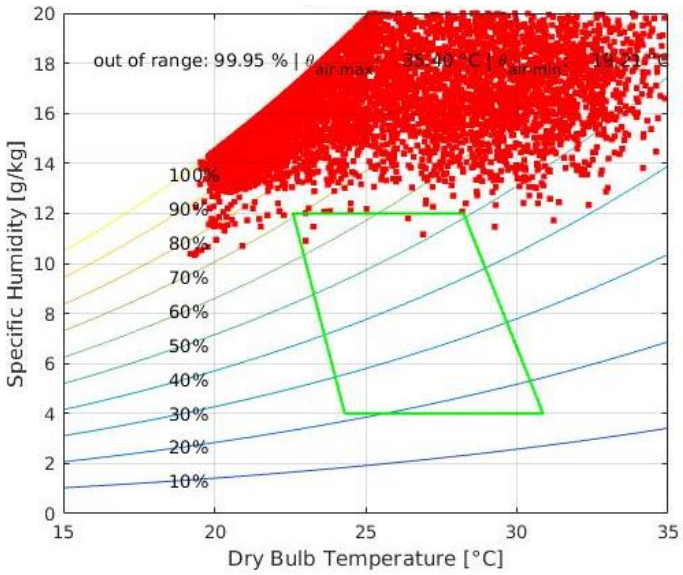

Figure 30 Psychometric chart, Ashrae 55 adaptive comfort, MEWF, OS1

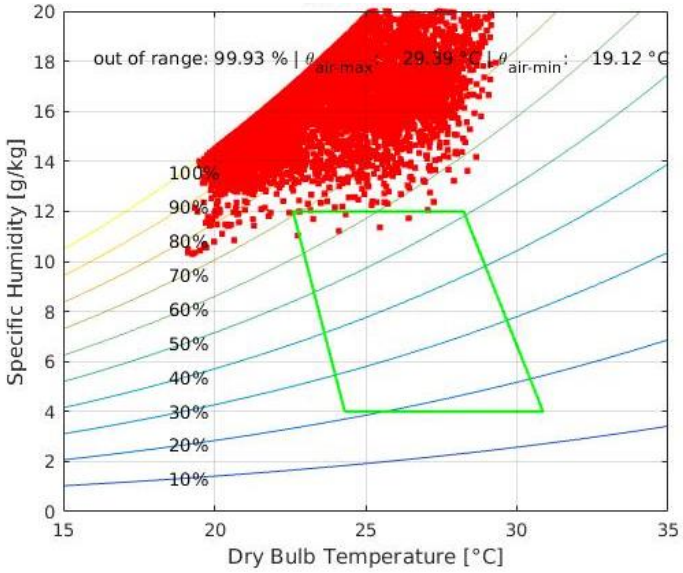

Figure 31 Psychometric chart, Ashrae 55 adaptive comfort, MEWF, OS2

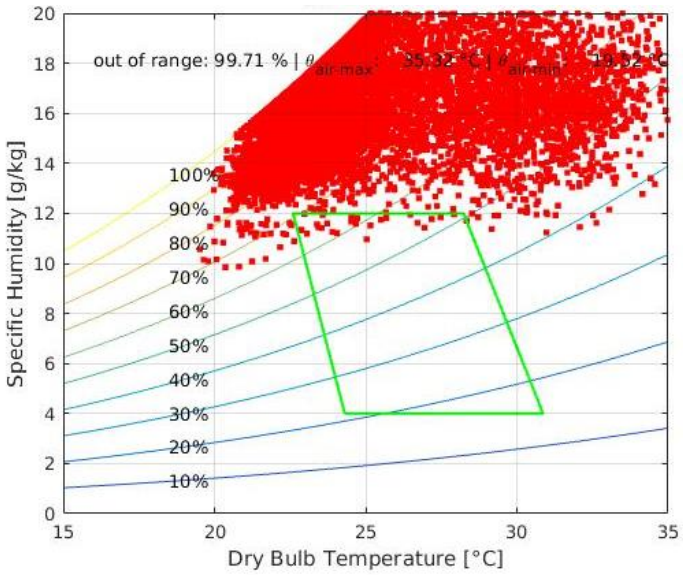

Figure 32 Psychometric chart, Ashrae 55 adaptive comfort, MEWF, OS3

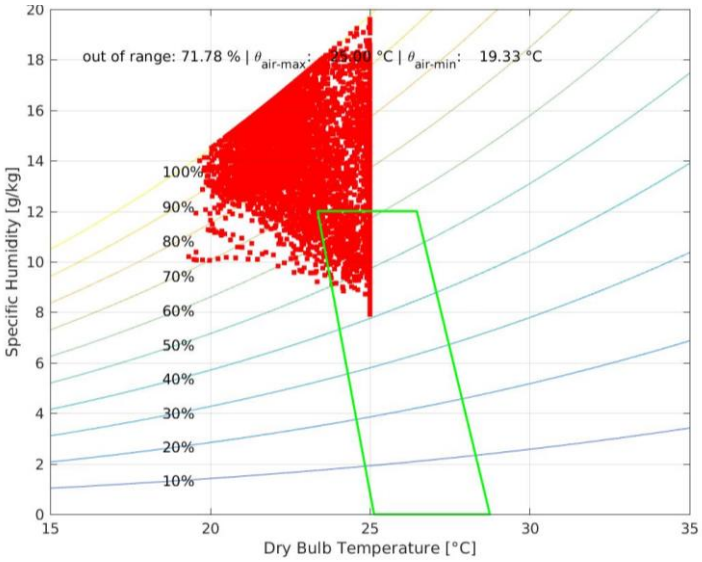

Figure 33 Psychometric chart, Ashrae standard 55, MEWF, OS4

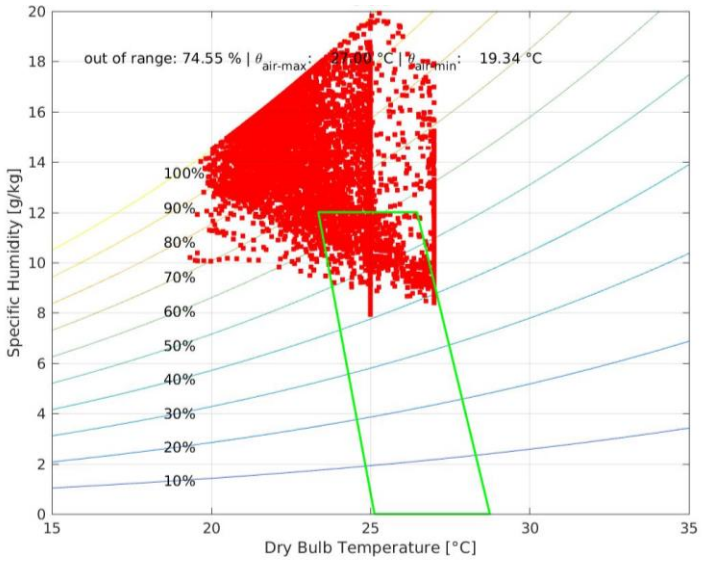

Figure 34 Psychometric chart, Ashrae standard 55, MEWF, OS5

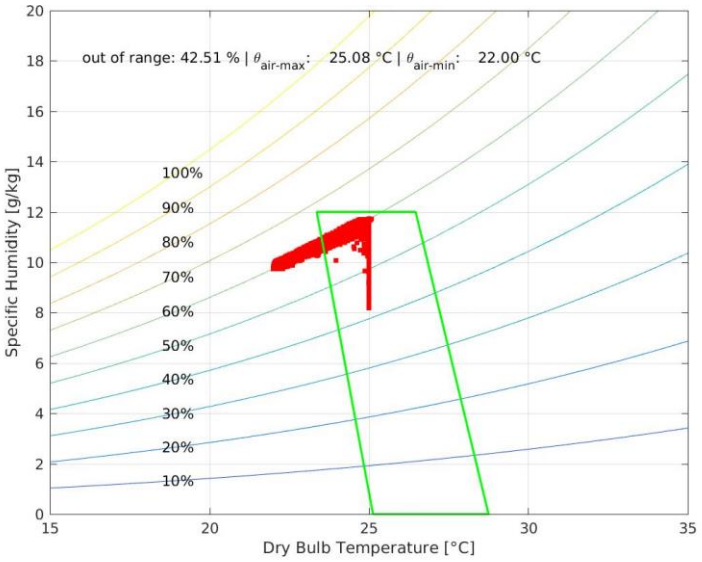

Figure 35 Psychometric chart, Ashrae standard 55, MEWF OS6

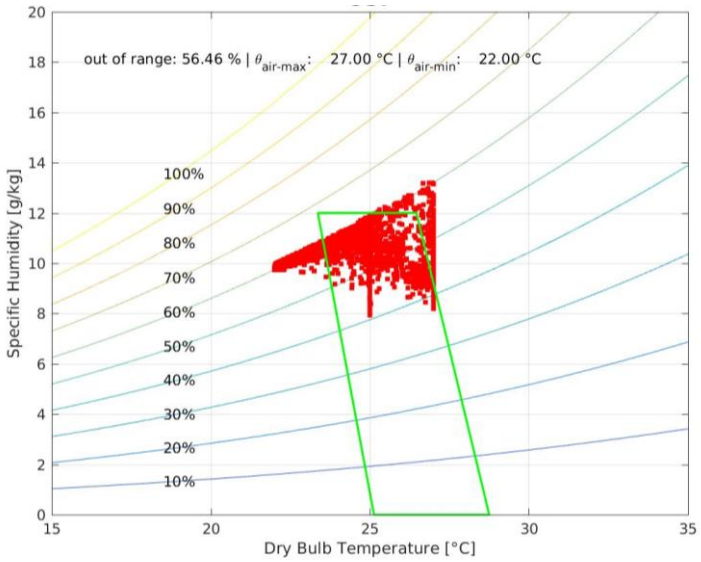

Figure 36 Psychometric chart, Ashrae standard 55, MEWF, OS7

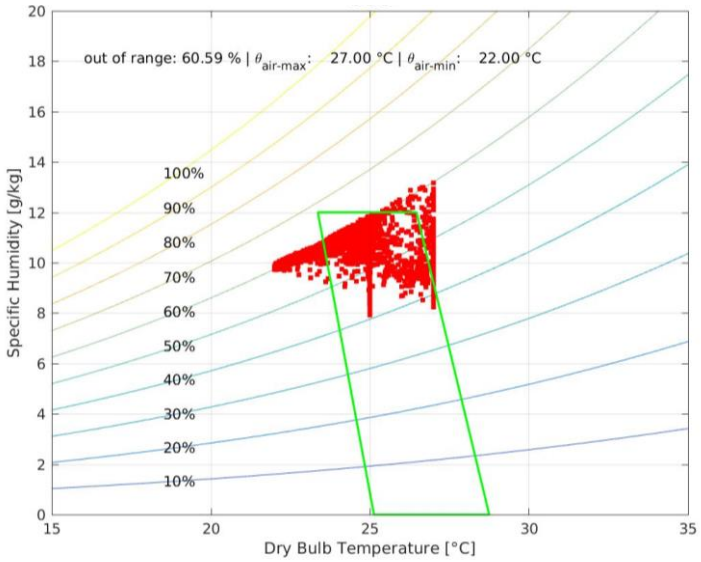

Figure 37 Psychometric chart, Ashrae standard 55, MEWF, OS8

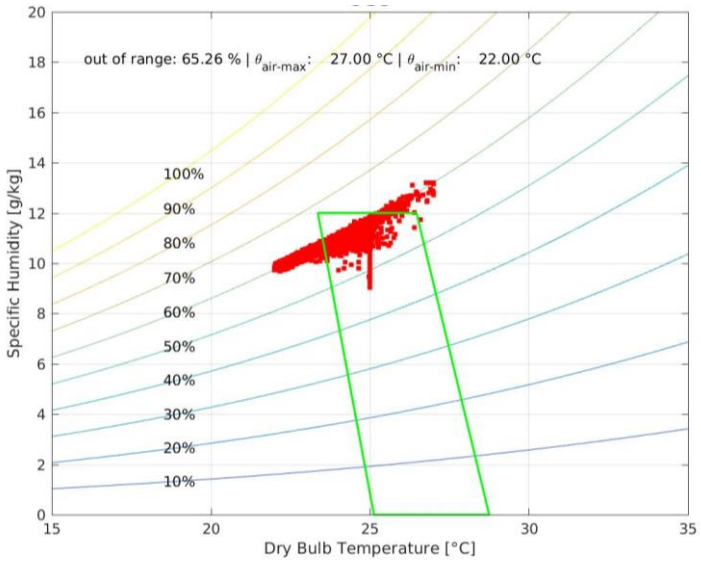

Figure 38 Psychometric chart, Ashrae standard 55, MEWF, OS9

3.2.2 Simulation with GLWF:

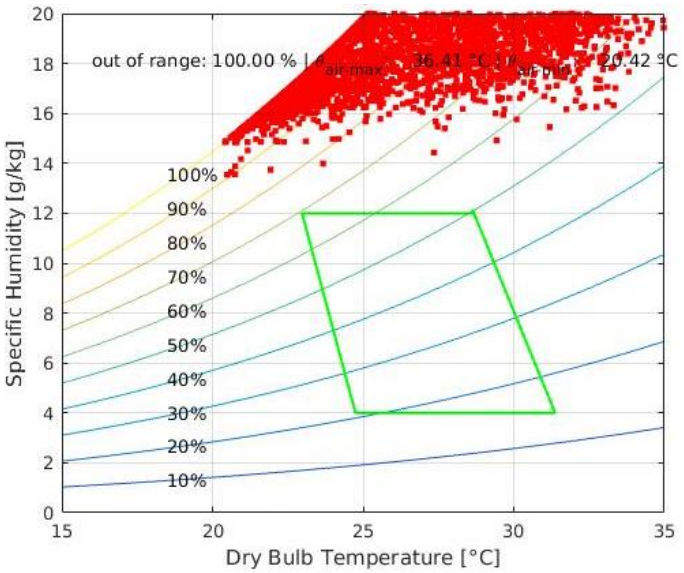

Figure 39 Psychometric chart, Ashrae 55 adaptive comfort, GLWF, BC2

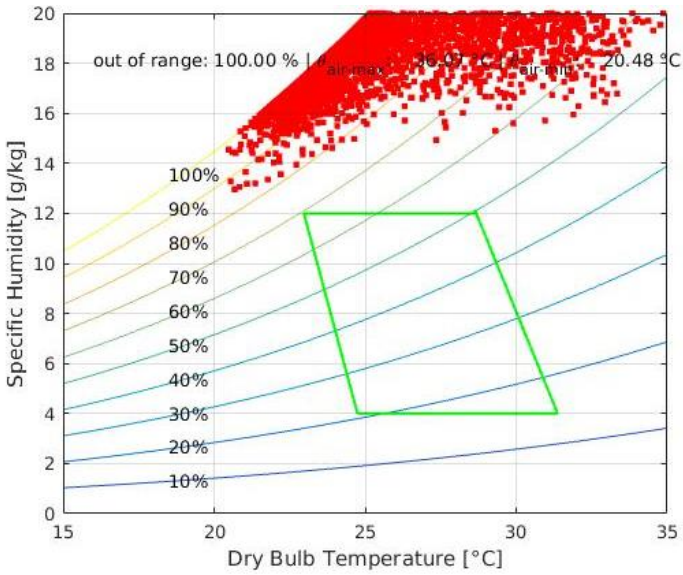

Figure 40 Psychometric chart, Ashrae 55 adaptive comfort, GLWF, OS3

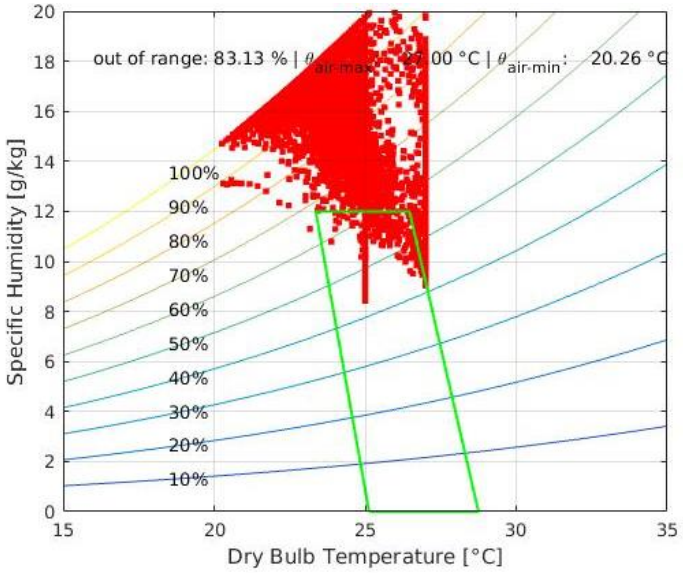

Figure 41 Psychometric chart, Ashrae standard 55, GLWF, OS5

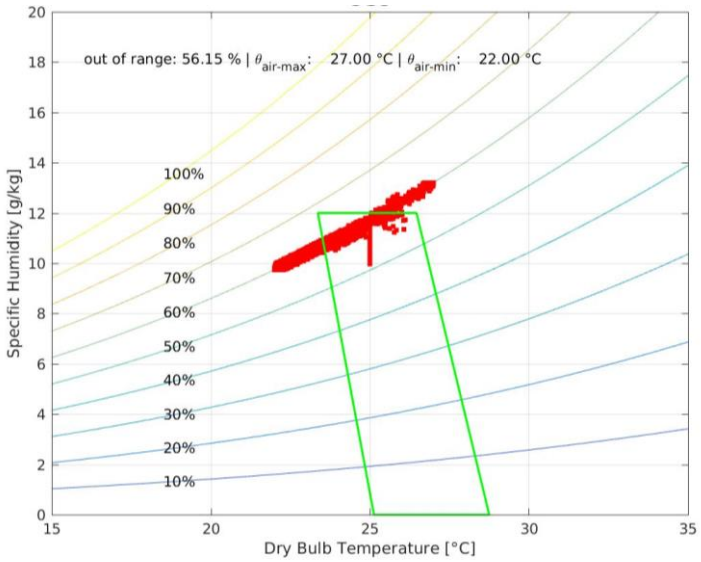

Figure 42 Psychometric chart, Ashrae standard 55, GLWF, OS9

3.2.3 Simulation with MOWF:

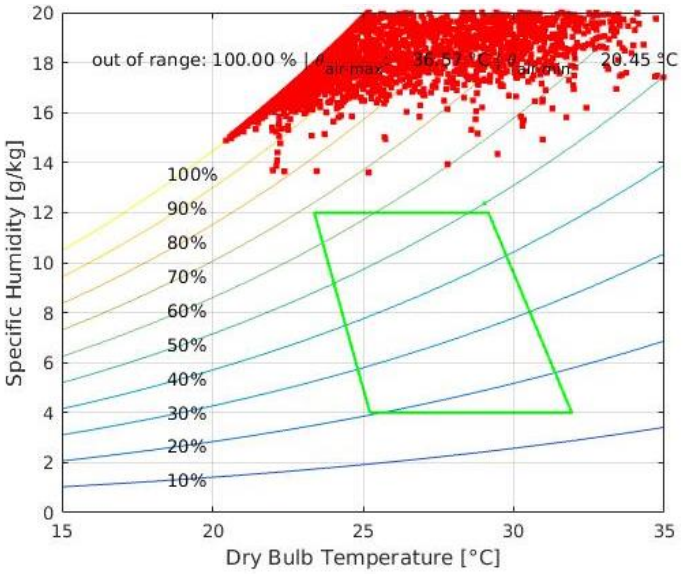

Figure 43 Psychometric chart, Ashrae 55 adaptive comfort, MOWF, BS2

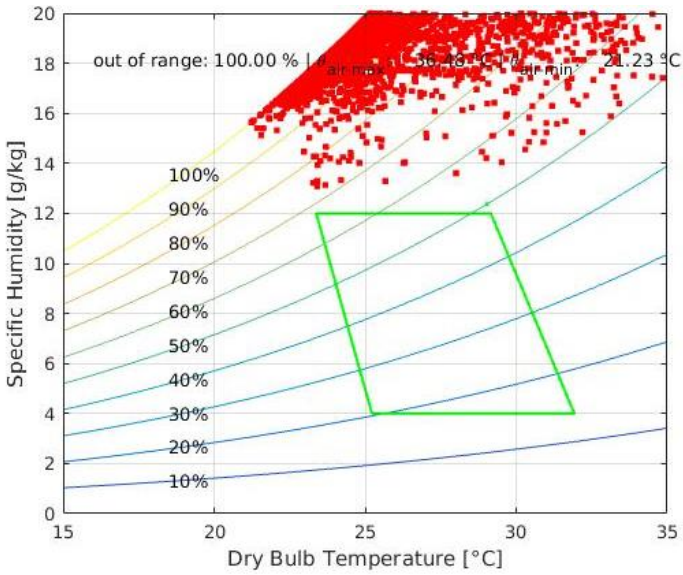

Figure 44 Psychometric chart, Ashrae standard 55, MOWF, OS3

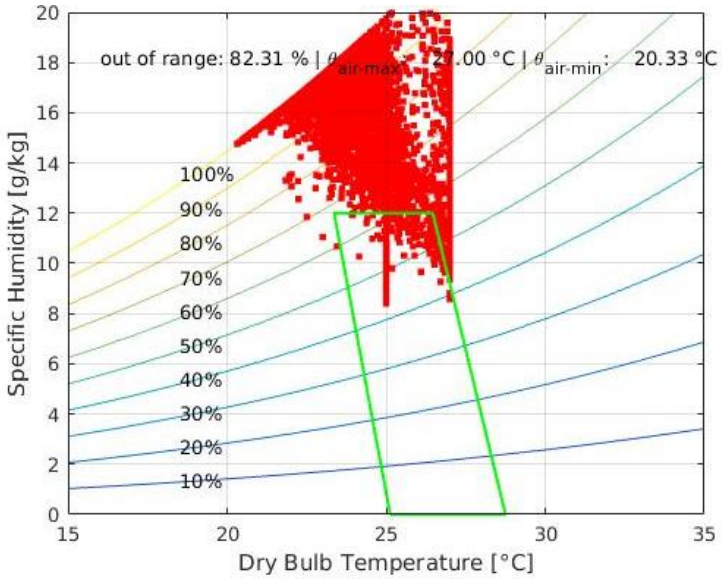

Figure 45 Psychometric chart, Ashrae standard 55, MOWF, OS5

Figure 46 Psychometric chart, Ashrae standard 55, MOWF, OS9

3.3 Overheating Index

The overheating index is defined as the sum of hourly temperature differences between the room temperature and an overheating reference temperature. For the purpose of this study as reference temperature the monthly upper limit of the acceptable comfort conditions according to Auliciems (1981) is used. Meaning the monthly neutrality temperature plus 2.5 °C. this provides 90% acceptability by the occupants according to the Ashrae standard 55.

$$OH = \sum_{i=1}^{n} \frac{\theta_i - \theta_{ref}}{n} \qquad (2)$$

OH $Overheating\ Index$

θ_i $Houly\ indoor\ temperatur\ in$ ℃

θ_{ref} $overheating\ refernce\ temperature\ in$ ℃

3.3.1 Simulation with MEWF:

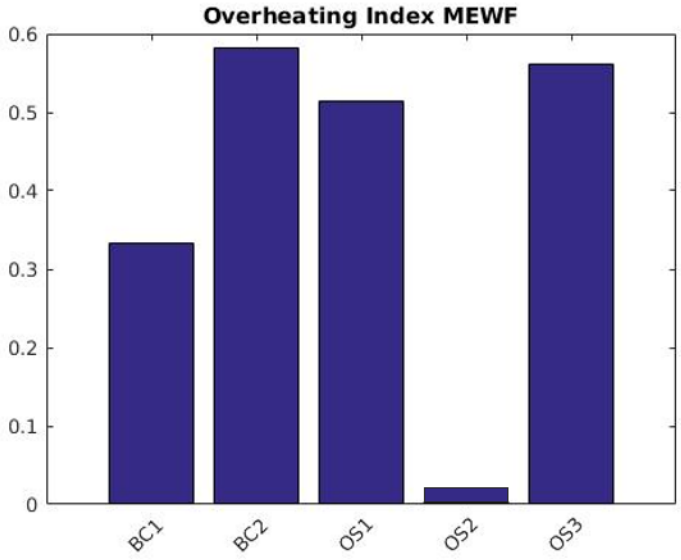

Figure 47 Comparison Overheating Index, MEWF

3.3.2 Simulation BC1:

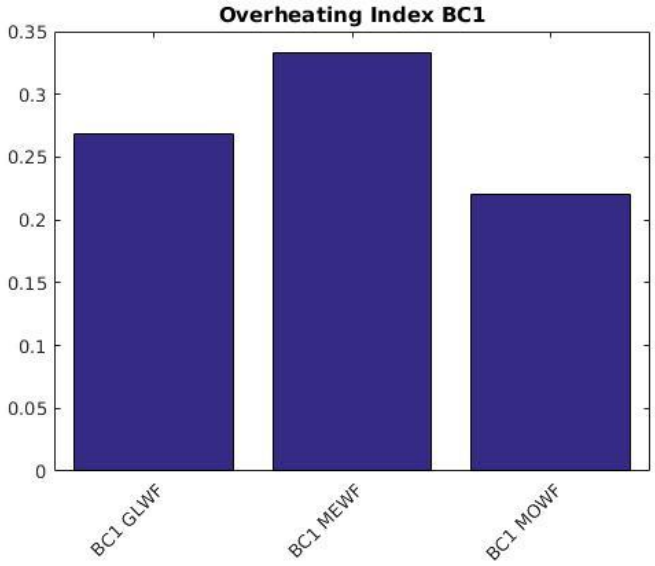

Figure 48 Comparison Overheating Index, BC1

3.3.3 Simulation OS3:

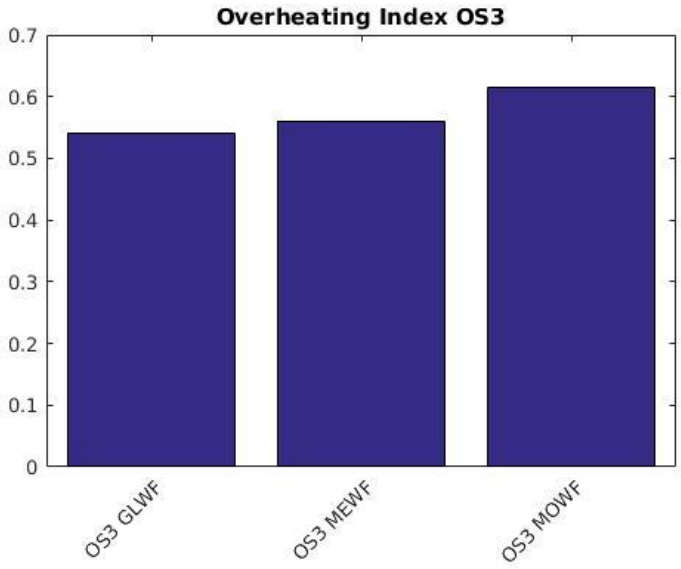

Figure 49 Comparison Overheating Index, OS3

3.4 Cooling Load

In this chapter the cooling loads of the scenarios where active cooling is used will be compared.

The cooling load indicates the rate at which the latent and sensible heat must be removed in order to maintain a constant indoor air temperature and humidity.

The cooling load is given in kWh on an annual basis per square meter, the peak values in Watt per square meter.

3.4.1 Simulation with MEWF:

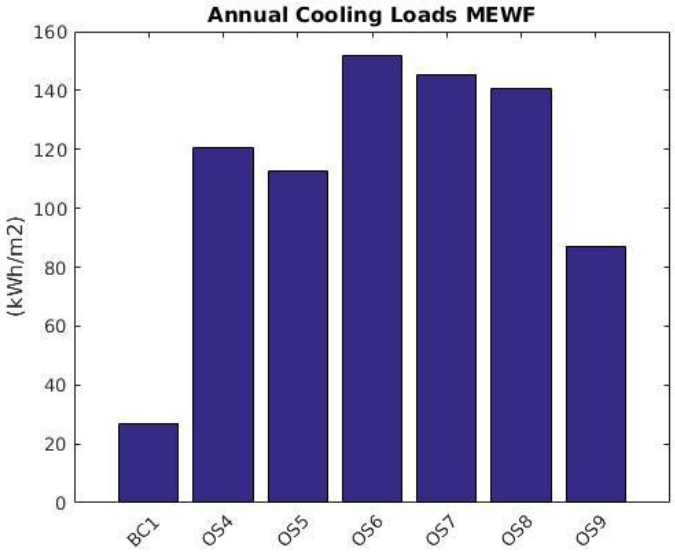

Figure 50 Comparison Annual Cooling Load MEWF

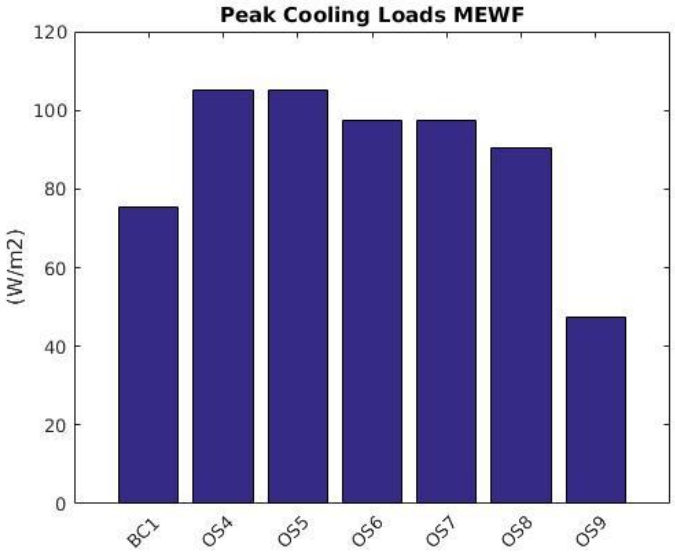

Figure 51 Comparison Peak Cooling Loads, MEWF

3.4.2 Simulation BC1:

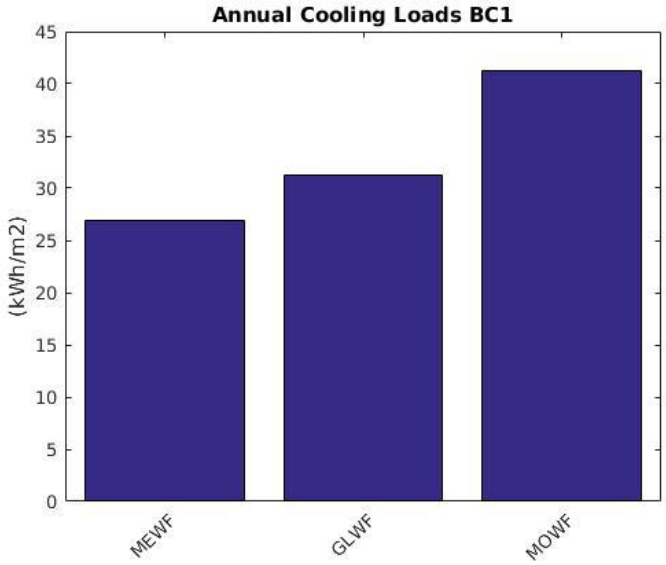

Figure 52 Comparison Annual Cooling Load, BC1

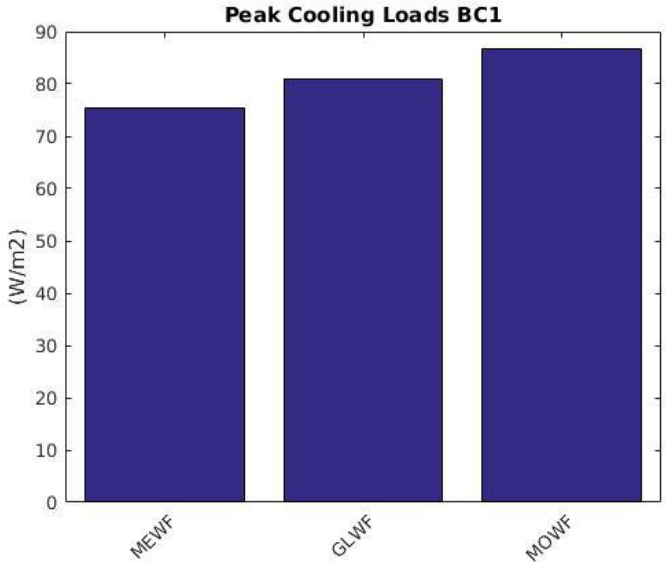

Figure 53 Comparison Peak Cooling Loads, BC1

3.4.3 Simulation OS6:

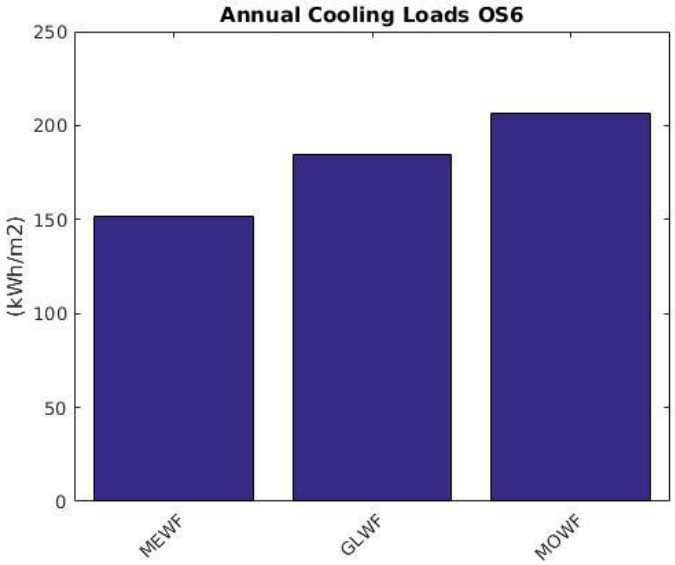

Figure 54 Comparison Annual Cooling Load, OS6

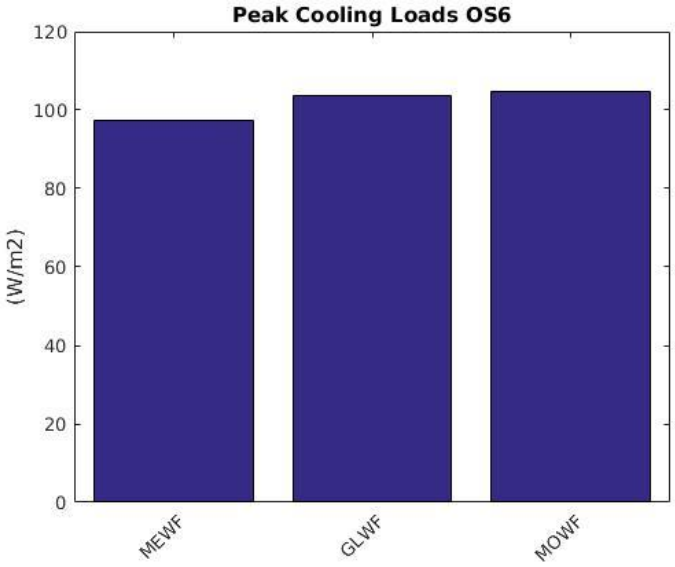

Figure 55 Comparison Peak Cooling Loads, OS6

3.4.4 Simulation OS9:

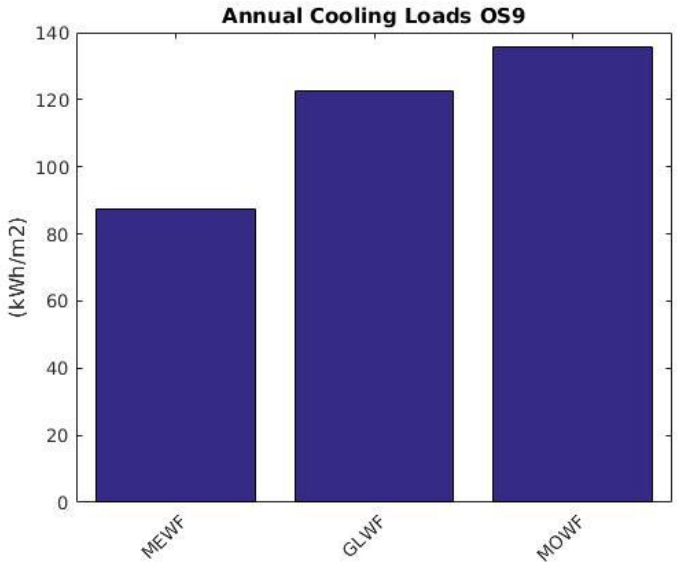

Figure 56 Comparison Annual Cooling Load, OS9

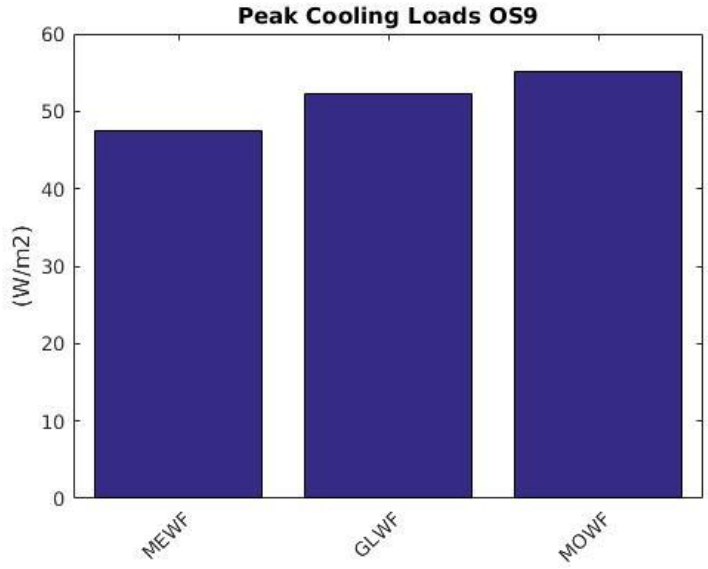

Figure 57 Comparison Peak Cooling Loads, OS9

4 DISCUSSION

4.1 Overview

In this chapter the results shown in 3 will be analyze and evaluated focusing three different criteria. In the first part 4.2 the passive cooling strategies will be compared regarding thermal comfort. Then, in chapter 4.3 the overheating index will be analyzed. In the last part 4.4 the active cooling strategies will be compared regarding the annual cooling loads and peak cooling loads.

The results will be analyzed in order to answer the following questions:

1. Are passive cooling strategies sufficient to provide thermal comfort?
2. How much overheating occurs when different design strategies are used?
3. How is the thermal comfort and overheating affected by the choice of the weather file?
4. To what extent do the different optimization strategies with active cooling influence the annual cooling load and the peak cooling load?
5. How is the cooling load affected by the choice of different weather files?

4.2 Thermal comfort

As presented in Figure 28 and Figure 29, the thermal comfort charts show that the indoor temperature and humidity of two base cases BC1 and BC2 lies both outside the comfort zone for more than 99% of the time. Although, in BC1, where active cooling is used the maximum air temperature drops slightly from 34.24 °C to 35.70°C.

Moreover, the passive cooling strategies OS1, OS2 and OS3 show that the indoor conditions are most of the time out of the comfort range: The optimization scenario with added insulation OS1 (Figure 30) shows no improvement compared to the base case. The optimization scenario with the white roof OS2 (Figure 31) shows the most significant change of the passive cooling strategies. Although the temperature and humidity are still out of the comfort range for over 99% of the time. However, the maximum air temperature drops from 35.70°C to 29.39°C compared to the base case with no passive cooling BC2. The third passive optimization scenario OS3 uses night time ventilation the psychometric chart shows that temperature and humidity do not change significantly compared to the base case and the data is still 99% of the time out of the comfort range (Figure 32).

The scenarios where active cooling but no dehumidification is used OS4-OS5 (Figure 33, Figure 34) show that the temperature drops but the data lies out of the comfort zone over 70% of the time due to the still high humidity levels.

Due to the drop in humidity in the scenarios were active cooling and dehumidification is used (OS6 and OS7) the data lies out of the comfort range below 57% of the time (Figure 35, Figure 36).

The psychometric chart of the last two scenarios where passive and active cooling are mixed (OS8 and OS9), show that the humidity lies about 60-65% of the time out of the comfort range (Figure 37, Figure 38).

To answer the question if the passive cooling strategies are sufficient to provide thermal comfort, the result show that, although all passive cooling strategies lower the temperature, acceptable thermal comfort cannot be provided as a consequence of the high humidity which cannot be removed by any passive cooling strategy.

The psychometric chart of results of the simulations runs with the weather file which includes a global warming scenario (GLWF) shows that due to the higher temperature and humidity the data lies 100% of the time outside of the comforts zone in the base case without active cooling BC2 (Figure 39) as well as the passive cooling scenarios OS3 (Figure 40). This is caused by the higher outdoor temperature and humidity of the weather file.

The scenarios with active cooling OS5 (Figure 41) and dehumidification scenarios OS9 (Figure 42) do not show hardly any difference compared to the results of the simulation with the weather file generated with meteonorm.

Furthermore, when comparing the psychometric chart of the base case simulated with the modified weather file (MOWF) (Figure 43) to the one simulated with the global warming (GLWF) it has similar results. As shown in Figure 44 the results of OS3 simulated with MOWF shows a slightly lower humidity than simulated with GLWF, however it still remains 100% of the time outside the comfort zone.

As expected, the active cooling and dehumidification scenarios simulated with MOWF show hardly any difference compared to the results of the simulation runs with GLWF and MEWF.

Summarizing the results in the psychometric charts, it can be said that the influence of the weather file is substantial when considering the thermal comfort of passive cooling scenarios, while it is negligible when considering active cooling or dehumidification scenarios.

4.3 Overheating Index

The graph of the overheating Index (Figure 47) shows that the scenario where most overheating occurs is the base case with no active cooling, followed by OS3 and OS1. The scenario where least overheating occurs is OS2.

Figure 48 shows the comparison of the overheating index for different weather files and the simulation run BC1. All three results are around 0.3. The highest result shows the simulation with MEWF and the lowest the simulation with MOWF.

In Figure 49 the results of the overheating index of the simulation of OS3 are compared. The results do not change significantly when changing the weather file. This time the simulation with OS3 shows the highest results and the simulation with GLWF the lowest.

4.4 Cooling Load

Figure 50 displays the comparison of cooling loads of the scenarios where active cooling is used. It shows that the base case (BC1), is the scenario with the lowest cooling load with 27 kWh/m^{2}a. This is a consequence of the HVAC system with limited capacity. As expected, the scenarios where dehumidification is used (OS6, OS7) compared to the scenarios with just cooling (OS4, OS5) cause a raise in cooling demand about 30 kWh/m^{2}a. The scenarios where a varying cooling setpoint (OS5, OS6) is used have an about 7 kWh/m^{2}a lower annual cooling load compared to the ones with a constant cooling setpoint.

The two scenarios where active cooling and dehumidification is combined with passive cooling strategies, show that the impact of the annual cooling load is rather limited when insulation is used (OS8). The annual cooling load is still high with 140 kWh/m^{2}a. However, where active cooling is combined with a white roof (OS9) the cooling load drops to 87 kWh/m^{2}a, which is the lowest cooling load of all optimization cases.

Figure 51 shows the comparison of the peak cooling load. It is clear that there is no difference between varying and constant setpoint.

The scenario OS9 has the lowest peak cooling load with 47 W/m. Thus, the scenario OS9 has the lowest annual and peak cooling loads.

To investigate on the influence of different weather files on the cooling loads, Figure 52 shows the comparison of the simulation runs of the base case (BC1) with different weather files. The annual cooling load is the highest with 41 kWh/m^{2}a in the simulation run with the modified weather file MOWF. While the cooling load in the simulation with GLWF is about 24% smaller and in case of the MEWF about 40% smaller compared to MOWF (Figure 53).

The comparison of the peak cooling loads for the base case is shown in Figure 53. The graph shows the same general tendency, the peak cooling load of the simulation with MOWF is the highest with 87 W/m^2. The simulation run with GLWF and MEWF are about 6% and 13% smaller respectively.

The cooling loads of the scenario OS6 with different weather files shows a similar picture (Figure 54): The simulation run with MEWF has the lowest annual cooling load with 151 kWh/m^{2}a. The run with GLWF has a about 21% higher one with 184 kWh/m^{2}a and the one with MOWF is about 35% higher with 206 kWh/m^{2}a.

Figure 56 and Figure 57 show the annual cooling loads and peak cooling loads of the simulation of OS9. Again, the highest annual as well as peak cooling load has the simulation with MOWF 136 kWh/m^{2}a. The simulation with GLWF is slightly lower with 123 kWh/m^{2}a and the lowest annual, as well as peak cooling load, has MEWF with 87 kWh/m^{2}a.

Simulations with the weather file MOWF show overall the highest cooling loads, while the simulations with GLWF are in average about 12% lower for the annual cooling load and about 3% for the peak cooling load. The lowest cooling loads have the simulations with MEWF where the annual cooling load is about 28% lower and the peak cooling load about 9% lower compared to the simulation with MOWF

.

5 CONCLUSION

In this thesis, a simple workflow was created to generate a building simulation model from the existing point cloud data.

This building simulation model was then used to analyse the thermal performance of the existing building. Different optimization possibilities and passive cooling strategies were explored to reduce the cooling demand.

The results were compared focusing on three different criteria. First, the scenarios were compared regarding thermal comfort. Then, all strategies were compared regarding overheating. In the last part, the cooling loads of the active cooling scenarios were compared. Moreover, the influence of the choice of weather file was analyzed.

The analysis of the thermal comfort showed that although most passive optimization scenarios could reduce the average indoor temperature, thermal comfort (as defined according to the adaptive comfort model) could not be achieved with passive cooling strategies only.

All passive cooling scenarios showed overheating but could reduce the overheating index compared to the base case. The scenario where a white roof was used showed the least amount of overheating and a reduction of the maximum indoor temperature of 6K. However, it could not archive acceptable indoor conditions as the relative humidity rose up to 100% due to the lower air temperature.

The optimization scenarios where active cooling was used increased the cooling load compared to the base case. This can be explained by the HVAC system with limited capacity used in the base case. The change to a higher setpoint temperature during non-operating hours could decrease the annual cooling loads 6%. Thermal comfort could only be achieved by cooling and dehumidification which increased again the cooling loads about 27% compared to cooling only.

The combination of passive and active cooling strategies showed that especially the implementation of a white roof together with the active system could reduce the cooling load while providing thermal comfort. The cooling load dropped about 40% compared to the scenario with only dehumidification and cooling.

The influence of different weather files is substantial when considering thermal comfort as well as the cooling load. A difference of up to 28% in annual cooling load was found. For the peak cooling load, it has hardly any influence.

6 INDEX

6.1 List of Figures

Figure 1 Site plan, Affandi Museum
Figure 2 Affandi Museum (source: Ulrike Herbig, 2016)
Figure 3 Gallery 1, laser scan (source:
http://potree.org/demo/tuwien_baugeschichte/examples/museum_affandi.html)
Figure 4 Gallery I (source: Ulrike Herbig, 2016)
Figure 5 Workflow
Figure 6 Revit 2016, floor plan with point cloud
Figure 7: Revit 2016, BIM geometry model, before exporting
Figure 8 Open Studio, geometry model, after importing via gbXML
Figure 9 Open Studio, final geometry model
Figure 10 Open Studio, final geometry model with shading
Figure 11 Temperature range in Yogyakarta, meteonorm weather file,
Figure 12 Absolute humidity range in Yogyakarta, meteonorm weather file
Figure 13 Koeppen Geiger map (source: http://koeppen-geiger.vu-wien.ac.at)
Figure 14 Sensor location in the Affandi museum
Figure 15 Sensor Location Gallery 1
Figure 16 Sensor data, temperature
Figure 17 Sensor data, absolute humidity
Figure 18 Psychometric Chart, ASHRAE 55, Gallery 1
Figure 19: Sensor location, Gallery 1
Figure 20 Mean hourly temperature distribution for a reference day
Figure 21 Comparison measured data and weather files
Figure 22 Comparison measured data and weather files
Figure 23 Cross section, Gallery I
Figure 24 Ground floor, Gallery I
Figure 25 Gallery I, Skylight (source: Ulrike Herbig, 2016)
Figure 26 Gallery I, closed window (source: Ulrike Herbig, 2016)
Figure 27 Weather files, mean hourly temperature distribution for a reference day
Figure 28 Psychometric chart, Ashrae standard 55, MEWF, BC1
Figure 29 Psychometric chart, Ashrae 55 adaptive comfort, MEWF, BC2
Figure 30 Psychometric chart, Ashrae 55 adaptive comfort, MEWF, OS1
Figure 31 Psychometric chart, Ashrae 55 adaptive comfort, MEWF, OS2
Figure 32 Psychometric chart, Ashrae 55 adaptive comfort, MEWF, OS3

Figure 33 Psychometric chart, Ashrae standard 55, MEWF, OS4
Figure 34 Psychometric chart, Ashrae standard 55, MEWF, OS5
Figure 35 Psychometric chart, Ashrae standard 55, MEWF OS6
Figure 36 Psychometric chart, Ashrae standard 55, MEWF, OS7
Figure 37 Psychometric chart, Ashrae standard 55, MEWF, OS8
Figure 38 Psychometric chart, Ashrae standard 55, MEWF, OS9
Figure 39 Psychometric chart, Ashrae 55 adaptive comfort, GLWF, BC2
Figure 40 Psychometric chart, Ashrae 55 adaptive comfort, GLWF, OS3
Figure 41 Psychometric chart, Ashrae standard 55, GLWF, OS5
Figure 42 Psychometric chart, Ashrae standard 55, GLWF, OS9
Figure 43 Psychometric chart, Ashrae 55 adaptive comfort, MOWF, BS2
Figure 44 Psychometric chart, Ashrae standard 55, MOWF, OS3
Figure 45 Psychometric chart, Ashrae standard 55, MOWF, OS5
Figure 46 Psychometric chart, Ashrae standard 55, MOWF, OS9
Figure 47 Comparison Overheating Index, MEWF
Figure 48 Comparison Overheating Index, BC1
Figure 49 Comparison Overheating Index, OS3
Figure 50 Comparison Annual Cooling Load MEWF
Figure 51 Comparison Peak Cooling Loads, MEWF
Figure 52 Comparison Annual Cooling Load, BC1
Figure 53 Comparison Peak Cooling Loads, BC1
Figure 54 Comparison Annual Cooling Load, OS6
Figure 55 Comparison Peak Cooling Loads, OS6
Figure 56 Comparison Annual Cooling Load, OS9
Figure 57 Comparison Peak Cooling Loads, OS9

6.2 List of Tables

Table 1 Classification of Input Data
Table 2 Comparison weather files, mean monthly temperature °C
Table 3 Basic information, Gallery 1
Table 4 Characteristics of opaque constructions of the building envelope
Table 5 Characteristics of transparent constructions of the building envelope
Table 6 Optimization options

6.3 List of Equations

(1) Equation modified weather file 22
(2) Equation overheating index.....42

7 REFERENCES

Ashrae (Ed.), 2015. *ASHRAE Handbook. Heating, ventilating, and air-conditioning applications*. Atlanta: ASHRAE.

Auliciems, A., 1981. *Towards a psycho-physiological model of thermal perception*. International Journal of Biometeorology 25, pp. 109–122.

Dobelis, M., Kalinka and M., Borodinecs, A., 2016. *The Capture of BIM compatibile 3D Building Model from Laser Scan Data,* In: 17th International Conference on Geometry and Graphics (ICGG 2016), 4-8 August 2016, Bejing.

Feriadi, H. and Wong, N.H., 2004. *Thermal comfort for naturally ventilated houses in Indonesia*. Energy and Buildings 36, pp. 614–626.

Herbig, U., Styhler-Aydin, G., Grandits, D., Stampfer, L. and Pont, U. 2016 *The Architecture of the Affandi Museum. Approaches to a Piece of Art.*

Herbig, U., Styhler-Aydın, G., Grandits, D., Stampfer, L., Pont, U.; Mayer, I., 2017. *Digital Workflows for Restoration and Management of the Museum Affandi - a Case Study in Challenging Circumstances*. ISPRS - International Archives of the Photogrammetry, Remote Sensing and Spatial Information Sciences XLII-2/W5, pp. 329–334.

Hichri, N., Stefani, L., Luca, P. and de Hamon, G., 2013. *From Point Cloud to BIM: a Survey of existing Approaches.* In: XXIV International CIPA Symposium 2013, 2-6 September 2013, Strasbourg.

Imaginit: *IMAGINiT's Scan to BIM.* http://blogs.rand.com/architectural/scan-to-bim/. Accessed 4. 12. 2017.

Liping, W. and Hien, W.N., 2007. *The impacts of ventilation strategies and facade on indoor thermal environment for naturally ventilated residential buildings in Singapore.* Building and Environment 42, pp. 4006–4015.

Luo, M., Cao, B., Zhou, X.; Li, M., Zhang, J., Ouyang, Q. and Zhu, Y., 2014. *Can personal control influence human thermal comfort? A field study in residential buildings in China in winter*. Energy and Buildings 72, pp. 411–418.

Matsumoto, H., Tsuzuki, K. and Susanti, L., 2017. *Bioclimatic Analysis in Pre Design Stage of Passive House in Indonesia*. Buildings 2017 p. 24.

OECD; IEA, 2013. *Transition to Sustainable Buildings. Strategies and Opportunities to 2050.* Paris: OECD Publishing.

Pak, H.T., Pont, U. and Mahdavi, A., 2013. *Thermal performance of a test cell in a hot and humid climate: The impact of thermal insulation* In: 2nd Central European Symposium on Building Physics (CESBP 2013), 9 – 11 September 2013, Vienna.

De Deara, R. J. and Bragerb, G. S. 2002. *Thermal comfort in naturally ventilated buildings: revisions to ASHRAE Standard 55*. Energy and buildings, 34(6), pp. 549-561. DOI: 10.1016/S0378-7788(02)00005-1.

Tang, P., Huber, D., Akinci, B., Lipman, R. and Lytle, A., 2010. *Automatic reconstruction of as-built building information models from laser-scanned point clouds. A review of related techniques*. Automation in Construction 19, pp. 829–843.

Thomson, C. and Boehm, J., 2015. *Automatic Geometry Generation from Point Clouds for BIM.* Remote Sensing 7, pp. 11753–11775.

Turner, E., Cheng, P. and Zakhor, A., 2015. *Fast, Automated, Scalable Generation of Textured 3D Models of Indoor Environments*. IEEE Journal of Selected Topics in Signal Processing 9, pp. 409–421.

Urban, B. and Roth, K, 2010. Guidelines for Selecting Cool Roofs*. https://www.energy.gov/eere/femp/downloads/guidelines-selecting-cool-roofs* Accessed 5. 2. 2018).

8 APPENDIX

A. Psychometric charts

Simulation with GLWF

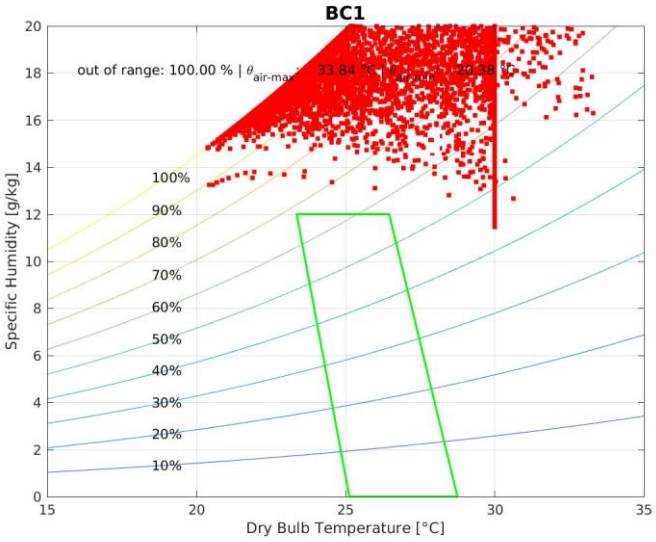

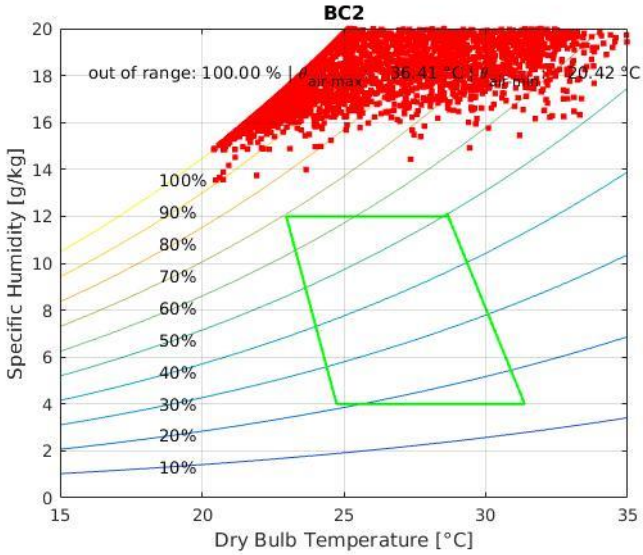

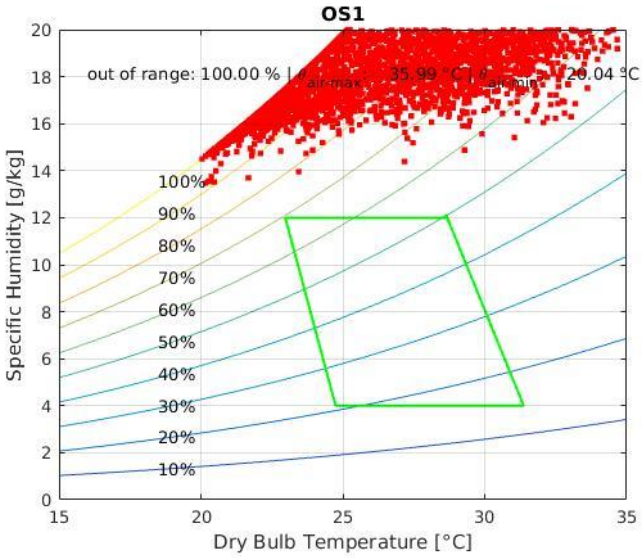
OS1
out of range: 100.00 % | $\theta_{air\,max}$: 35.99 °C | $\theta_{air\,min}$: 20.04 °C
Specific Humidity [g/kg]
Dry Bulb Temperature [°C]
100%
90%
80%
70%
60%
50%
40%
30%
20%
10%

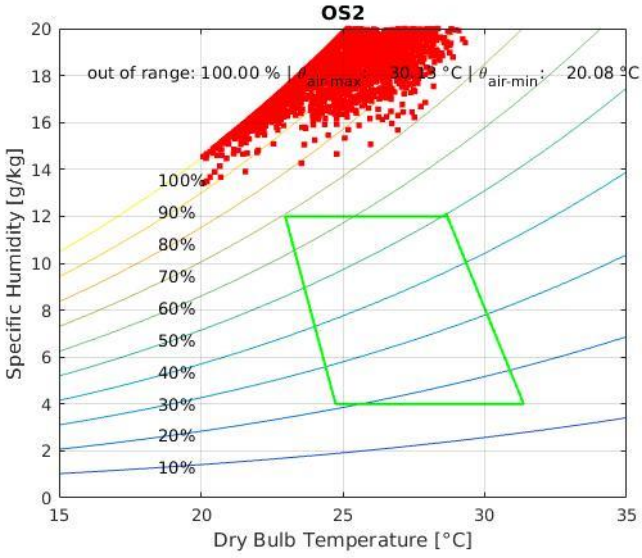
OS2
out of range: 100.00 % | $\theta_{air\,max}$: 30.13 °C | $\theta_{air\,min}$: 20.08 °C
Specific Humidity [g/kg]
Dry Bulb Temperature [°C]
100%
90%
80%
70%
60%
50%
40%
30%
20%
10%

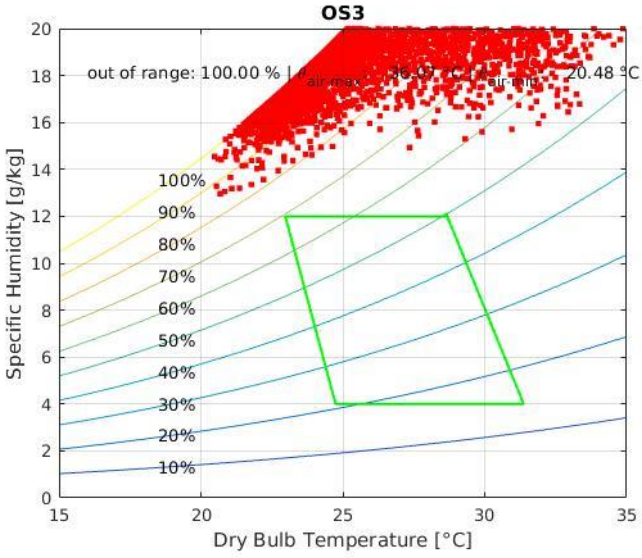
OS3
out of range: 100.00 % | $\theta_{air\,max}$: 30.07 °C | $\theta_{air\,min}$: 20.48 °C
Specific Humidity [g/kg]
Dry Bulb Temperature [°C]
100%
90%
80%
70%
60%
50%
40%
30%
20%
10%

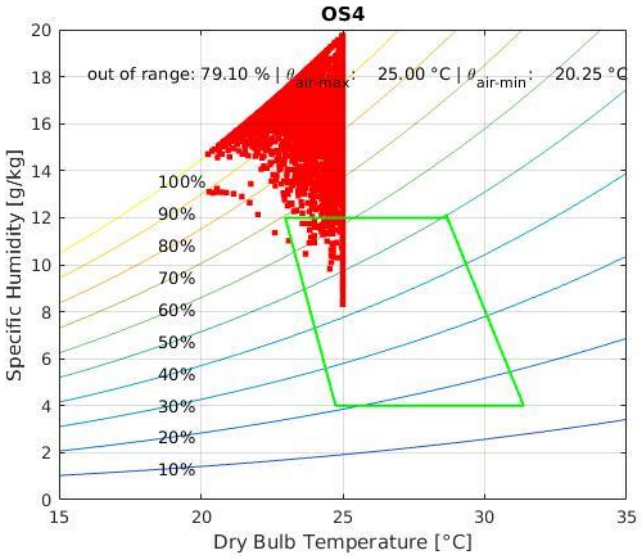
OS4
out of range: 79.10 % | $\theta_{air\text{-}max}$: 25.00 °C | $\theta_{air\text{-}min}$: 20.25 °C
Specific Humidity [g/kg]
Dry Bulb Temperature [°C]
100%
90%
80%
70%
60%
50%
40%
30%
20%
10%

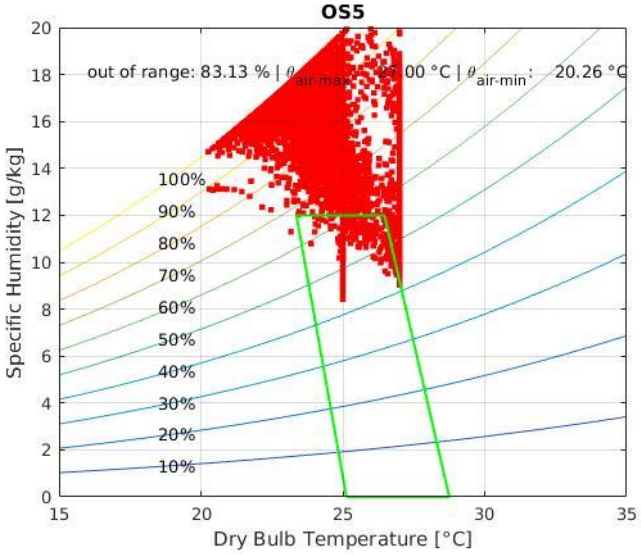
OS5
out of range: 83.13 % | $\theta_{air\text{-}max}$: 27.00 °C | $\theta_{air\text{-}min}$: 20.26 °C
Specific Humidity [g/kg]
Dry Bulb Temperature [°C]
100%
90%
80%
70%
60%
50%
40%
30%
20%
10%

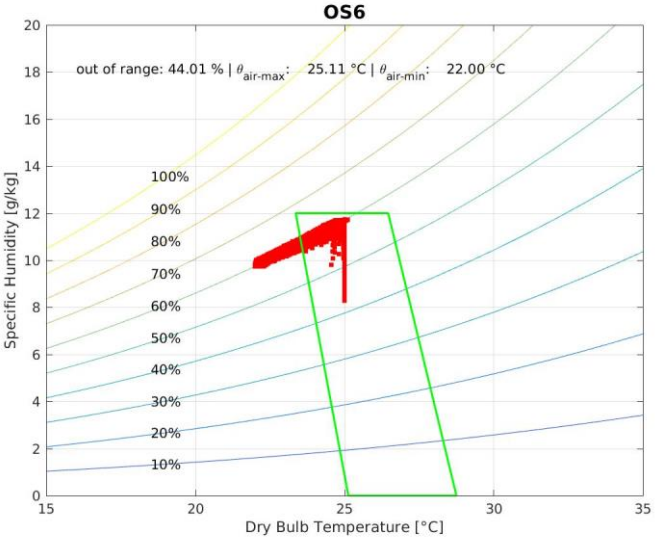
OS6
out of range: 44.01 % | $\theta_{air\text{-}max}$: 25.11 °C | $\theta_{air\text{-}min}$: 22.00 °C
Specific Humidity [g/kg]
Dry Bulb Temperature [°C]
100%
90%
80%
70%
60%
50%
40%
30%
20%
10%

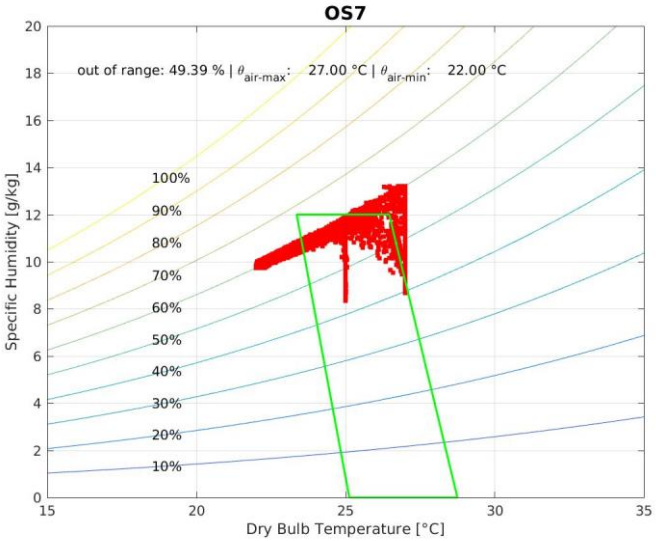
OS7
out of range: 49.39 % | $\theta_{air\text{-}max}$: 27.00 °C | $\theta_{air\text{-}min}$: 22.00 °C
Specific Humidity [g/kg]
Dry Bulb Temperature [°C]
100%
90%
80%
70%
60%
50%
40%
30%
20%
10%

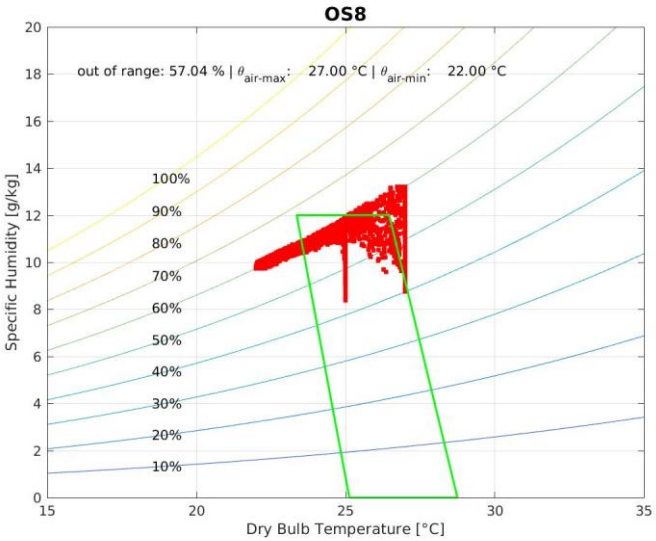
OS8
out of range: 57.04 % | $\theta_{air\text{-}max}$: 27.00 °C | $\theta_{air\text{-}min}$: 22.00 °C
Specific Humidity [g/kg]
Dry Bulb Temperature [°C]
100%
90%
80%
70%
60%
50%
40%
30%
20%
10%

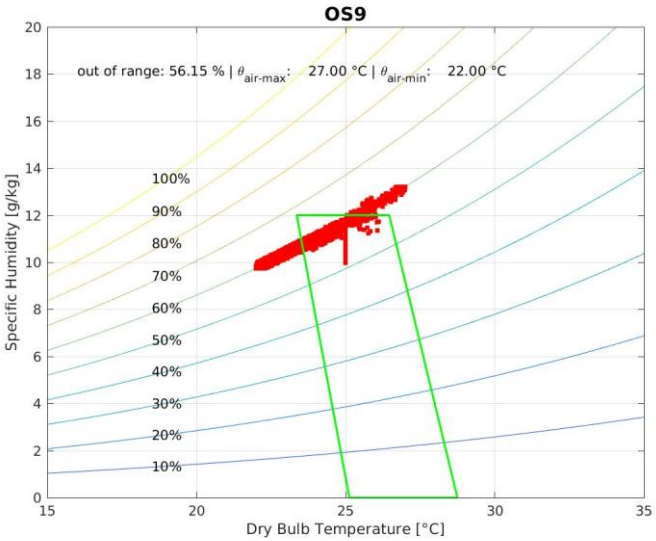
OS9
out of range: 56.15 % | $\theta_{air\text{-}max}$: 27.00 °C | $\theta_{air\text{-}min}$: 22.00 °C
Specific Humidity [g/kg]
Dry Bulb Temperature [°C]
100%
90%
80%
70%
60%
50%
40%
30%
20%
10%

Simulation with MOWF

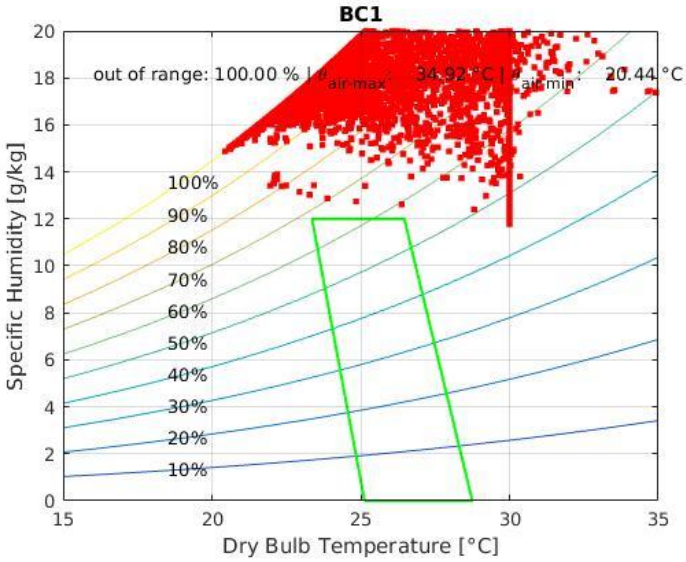

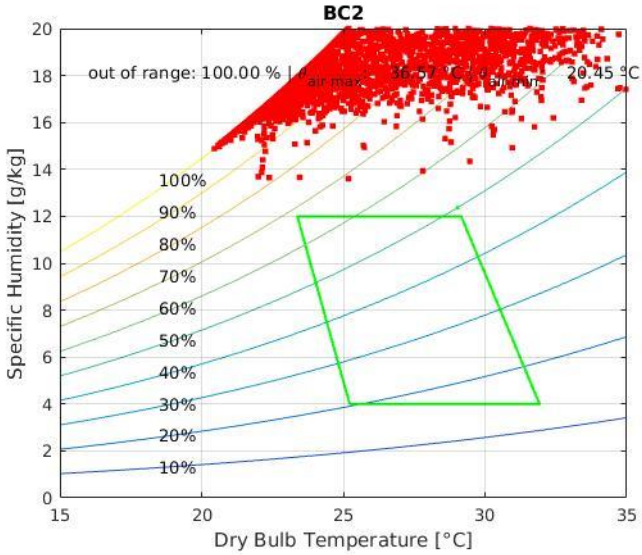

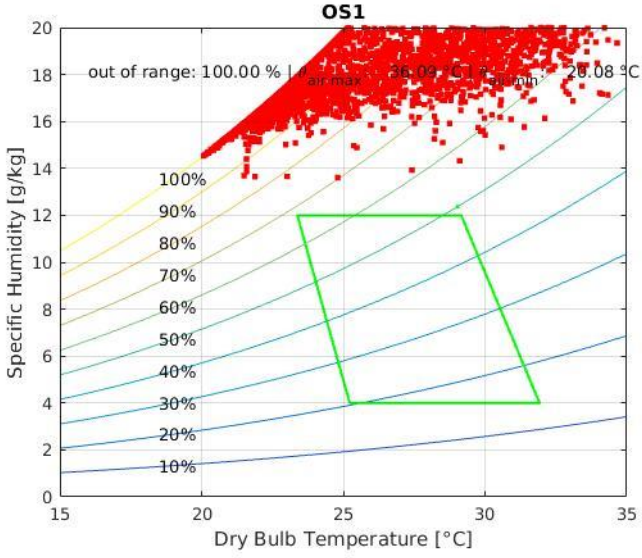

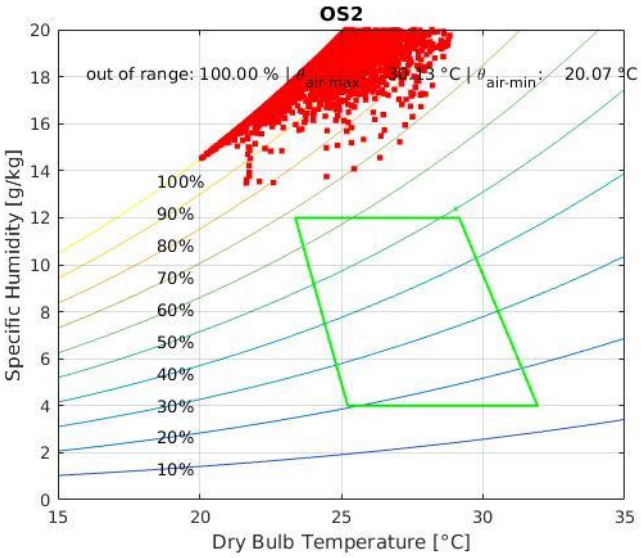
OS2
out of range: 100.00 % | $\theta_{air\text{-}max}$: 36.13 °C | $\theta_{air\text{-}min}$: 20.07 °C
Specific Humidity [g/kg]
Dry Bulb Temperature [°C]
100%
90%
80%
70%
60%
50%
40%
30%
20%
10%

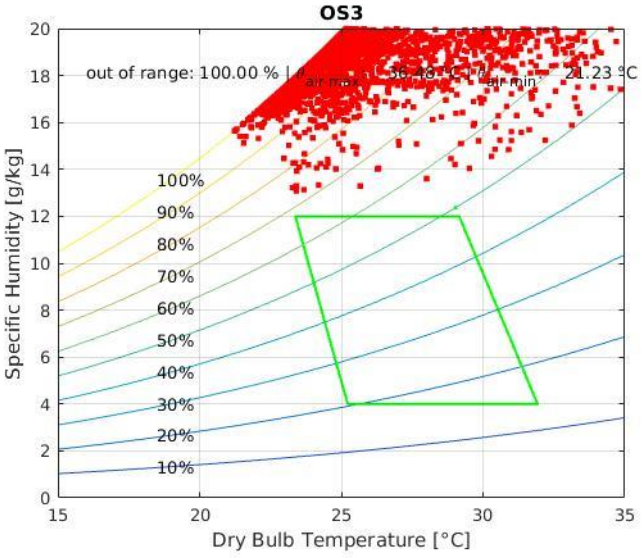
OS3
out of range: 100.00 % | $\theta_{air\text{-}max}$: 36.13 °C | $\theta_{air\text{-}min}$: 21.23 °C
Specific Humidity [g/kg]
Dry Bulb Temperature [°C]
100%
90%
80%
70%
60%
50%
40%
30%
20%
10%

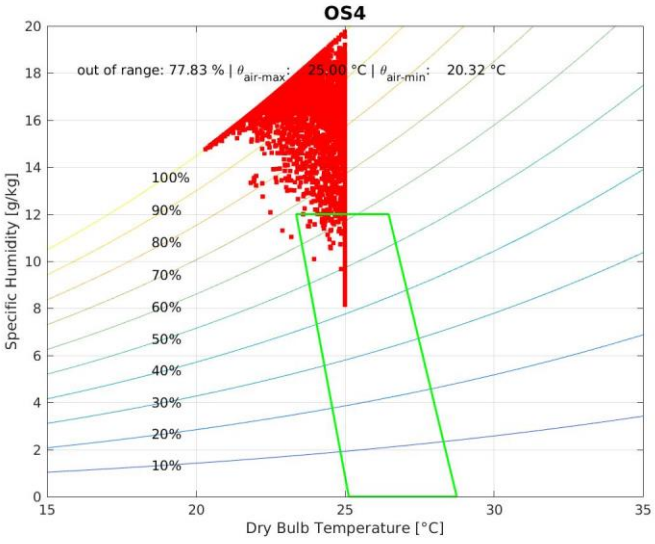
OS4
out of range: 77.83 % | $\theta_{air\text{-}max}$: 25.00 °C | $\theta_{air\text{-}min}$: 20.32 °C
Specific Humidity [g/kg]
Dry Bulb Temperature [°C]
100%
90%
80%
70%
60%
50%
40%
30%
20%
10%

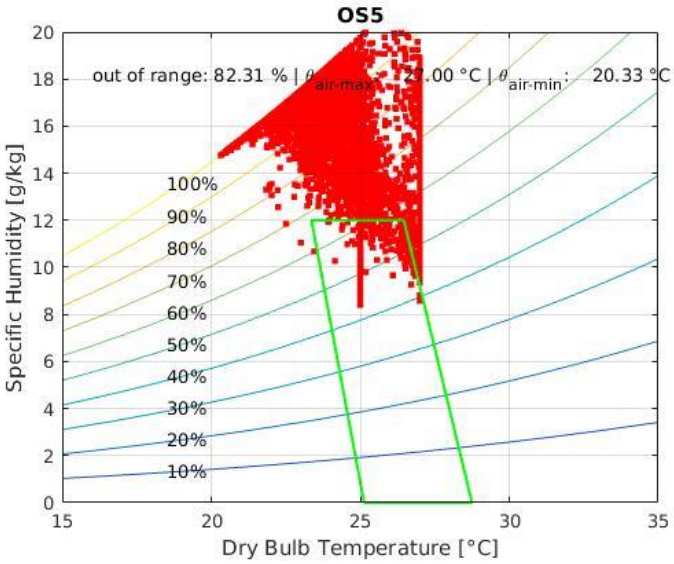
OS5
out of range: 82.31 % | $\theta_{air-max}$: 27.00 °C | $\theta_{air-min}$: 20.33 °C
Specific Humidity [g/kg]
Dry Bulb Temperature [°C]
100%
90%
80%
70%
60%
50%
40%
30%
20%
10%

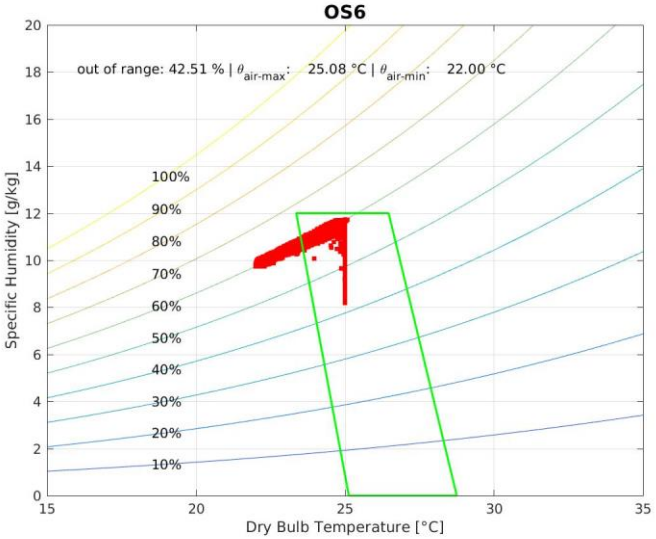
OS6
out of range: 42.51 % | $\theta_{air-max}$: 25.08 °C | $\theta_{air-min}$: 22.00 °C
Specific Humidity [g/kg]
Dry Bulb Temperature [°C]
100%
90%
80%
70%
60%
50%
40%
30%
20%
10%

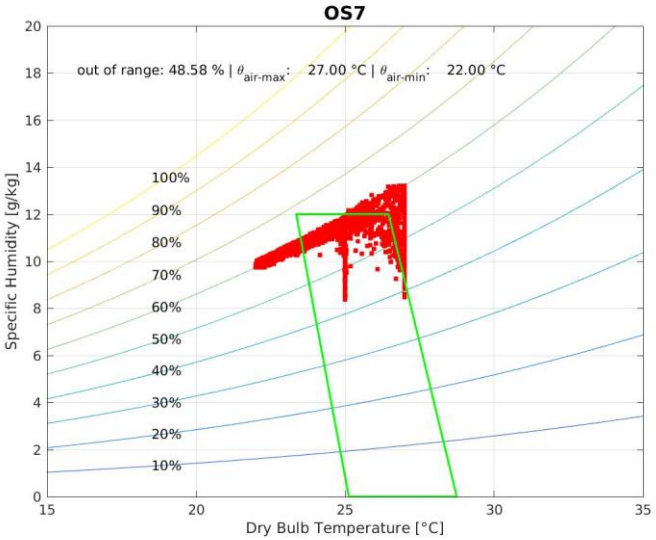
OS7
out of range: 48.58 % | $\theta_{air-max}$: 27.00 °C | $\theta_{air-min}$: 22.00 °C
Specific Humidity [g/kg]
Dry Bulb Temperature [°C]
100%
90%
80%
70%
60%
50%
40%
30%
20%
10%

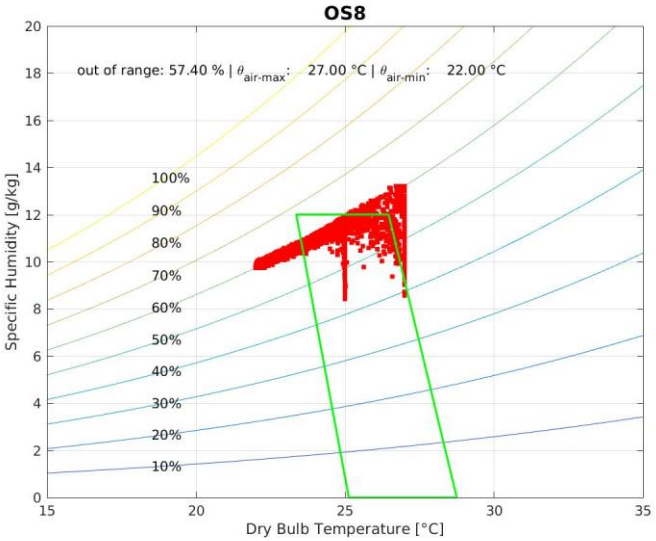
OS8
out of range: 57.40 % | $\theta_{air\text{-}max}$: 27.00 °C | $\theta_{air\text{-}min}$: 22.00 °C
Specific Humidity [g/kg]
Dry Bulb Temperature [°C]
100%
90%
80%
70%
60%
50%
40%
30%
20%
10%

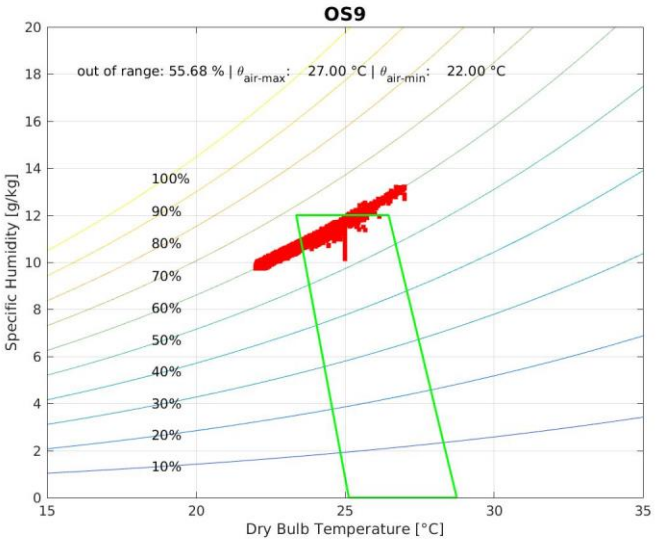
OS9
out of range: 55.68 % | $\theta_{air\text{-}max}$: 27.00 °C | $\theta_{air\text{-}min}$: 22.00 °C
Specific Humidity [g/kg]
Dry Bulb Temperature [°C]
100%
90%
80%
70%
60%
50%
40%
30%
20%
10%

B. Weather files

Meteonorm weather file MEWF:

MONTHLY MEANS	JAN	FEB	MAR	APR	MAY	JUN	JUL	AUG	SEP	OCT	NOV	DEC	
Global Horiz Radiation (Avg Hourly)	340	351	378	403	431	408	406	428	429	413	344	353	Wh/sq.m
Direct Normal Radiation (Avg Hourly)	203	185	214	268	383	399	324	319	290	240	178	199	Wh/sq.m
Diffuse Radiation (Avg Hourly)	196	220	223	217	181	159	200	213	221	234	217	210	Wh/sq.m
Global Horiz Radiation (Max Hourly)	1110	1046	1101	1072	954	890	885	956	1113	1057	1108	1094	Wh/sq.m
Direct Normal Radiation (Max Hourly)	990	924	1029	972	928	898	909	919	920	945	801	978	Wh/sq.m
Diffuse Radiation (Max Hourly)	488	540	537	491	428	423	442	466	520	544	532	532	Wh/sq.m
Global Horiz Radiation (Avg Daily Total)	4220	4313	4563	4765	5020	4719	4710	5039	5140	5031	4263	4404	Wh/sq.m
Direct Normal Radiation (Avg Daily Total)	2529	2279	2579	3173	4463	4616	3765	3747	3476	2934	2212	2483	Wh/sq.m
Diffuse Radiation (Avg Daily Total)	2430	2708	2695	2574	2116	1848	2328	2512	2650	2856	2685	2622	Wh/sq.m
Global Horiz Illumination (Avg Hourly)	38437	39848	42809	45447	48320	45554	45073	47475	47860	46379	39007	39985	lux
Direct Normal Illumination (Avg Hourly)	19145	15836	19314	23590	34955	36963	28552	27901	25426	21407	15411	18035	lux
Dry Bulb Temperature (Avg Monthly)	26	25	26	26	27	26	26	26	26	27	26	26	degrees C
Dew Point Temperature (Avg Monthly)	22	22	22	22	22	21	20	19	20	21	22	22	degrees C
Relative Humidity (Avg Monthly)	81	83	81	80	77	75	72	70	72	74	79	80	percent
Wind Direction (Monthly Mode)	260	270	250	250	100	60	80	180	180	160	250	290	degrees
Wind Speed (Avg Monthly)	1	1	1	1	1	1	1	2	1	1	1	1	m/s
Ground Temperature (Avg Monthly of 1 Depths)	26	26	26	26	26	26	26	26	26	26	26	26	degrees C

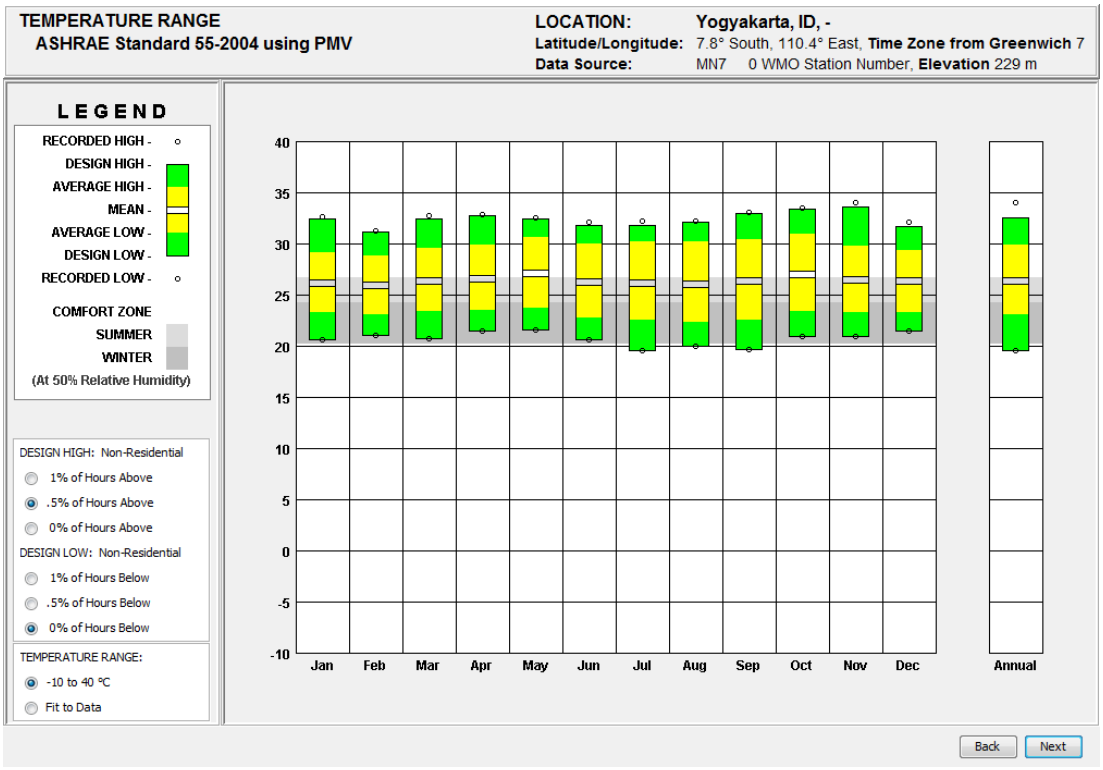

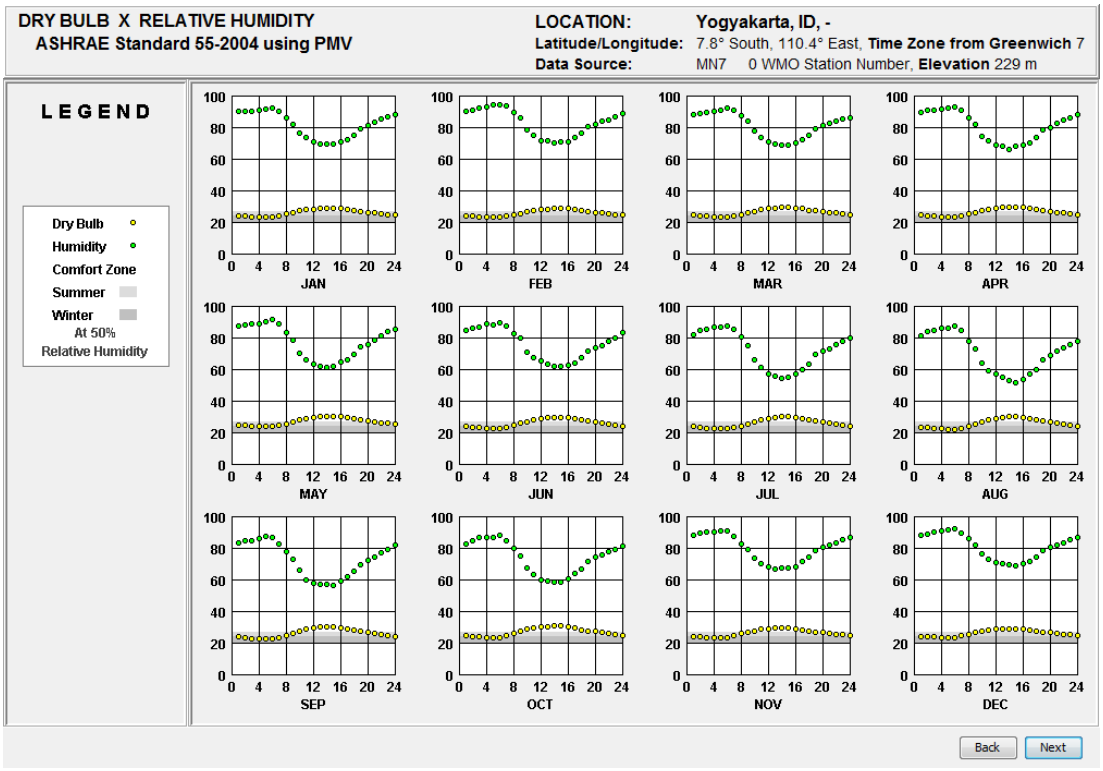

Global warming weather file GLWF:

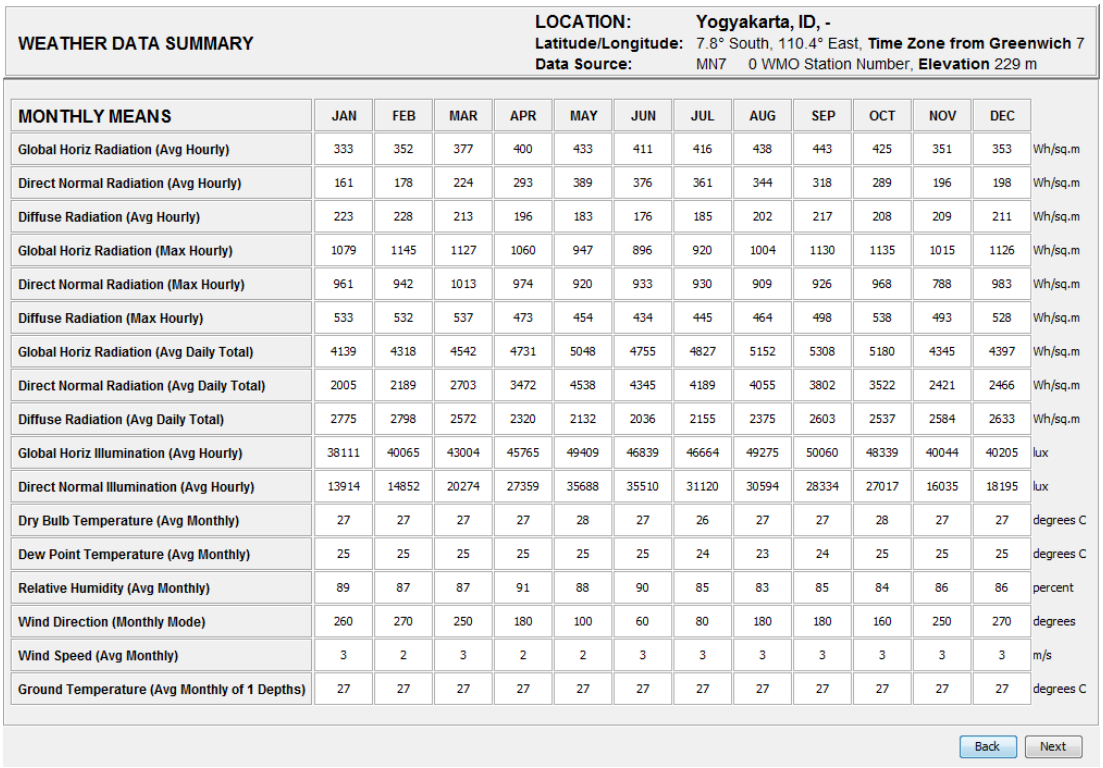

MONTHLY MEANS	JAN	FEB	MAR	APR	MAY	JUN	JUL	AUG	SEP	OCT	NOV	DEC	
Global Horiz Radiation (Avg Hourly)	333	352	377	400	433	411	416	438	443	425	351	353	Wh/sq.m
Direct Normal Radiation (Avg Hourly)	161	178	224	293	389	376	361	344	318	289	196	198	Wh/sq.m
Diffuse Radiation (Avg Hourly)	223	228	213	196	183	176	185	202	217	208	209	211	Wh/sq.m
Global Horiz Radiation (Max Hourly)	1079	1145	1127	1060	947	896	920	1004	1130	1135	1015	1126	Wh/sq.m
Direct Normal Radiation (Max Hourly)	961	942	1013	974	920	933	930	909	926	968	788	983	Wh/sq.m
Diffuse Radiation (Max Hourly)	533	532	537	473	454	434	445	464	498	538	493	528	Wh/sq.m
Global Horiz Radiation (Avg Daily Total)	4139	4318	4542	4731	5048	4755	4827	5152	5308	5180	4345	4397	Wh/sq.m
Direct Normal Radiation (Avg Daily Total)	2005	2189	2703	3472	4538	4345	4189	4055	3802	3522	2421	2466	Wh/sq.m
Diffuse Radiation (Avg Daily Total)	2775	2798	2572	2320	2132	2036	2155	2375	2603	2537	2584	2633	Wh/sq.m
Global Horiz Illumination (Avg Hourly)	38111	40065	43004	45765	49409	46839	46664	49275	50060	48339	40044	40205	lux
Direct Normal Illumination (Avg Hourly)	13914	14852	20274	27359	35688	35510	31120	30594	28334	27017	16035	18195	lux
Dry Bulb Temperature (Avg Monthly)	27	27	27	27	28	27	26	27	27	28	27	27	degrees C
Dew Point Temperature (Avg Monthly)	25	25	25	25	25	25	24	23	24	25	25	25	degrees C
Relative Humidity (Avg Monthly)	89	87	87	91	88	90	85	83	85	84	86	86	percent
Wind Direction (Monthly Mode)	260	270	250	180	100	60	80	180	180	160	250	270	degrees
Wind Speed (Avg Monthly)	3	2	3	2	2	3	3	3	3	3	3	3	m/s
Ground Temperature (Avg Monthly of 1 Depths)	27	27	27	27	27	27	27	27	27	27	27	27	degrees C

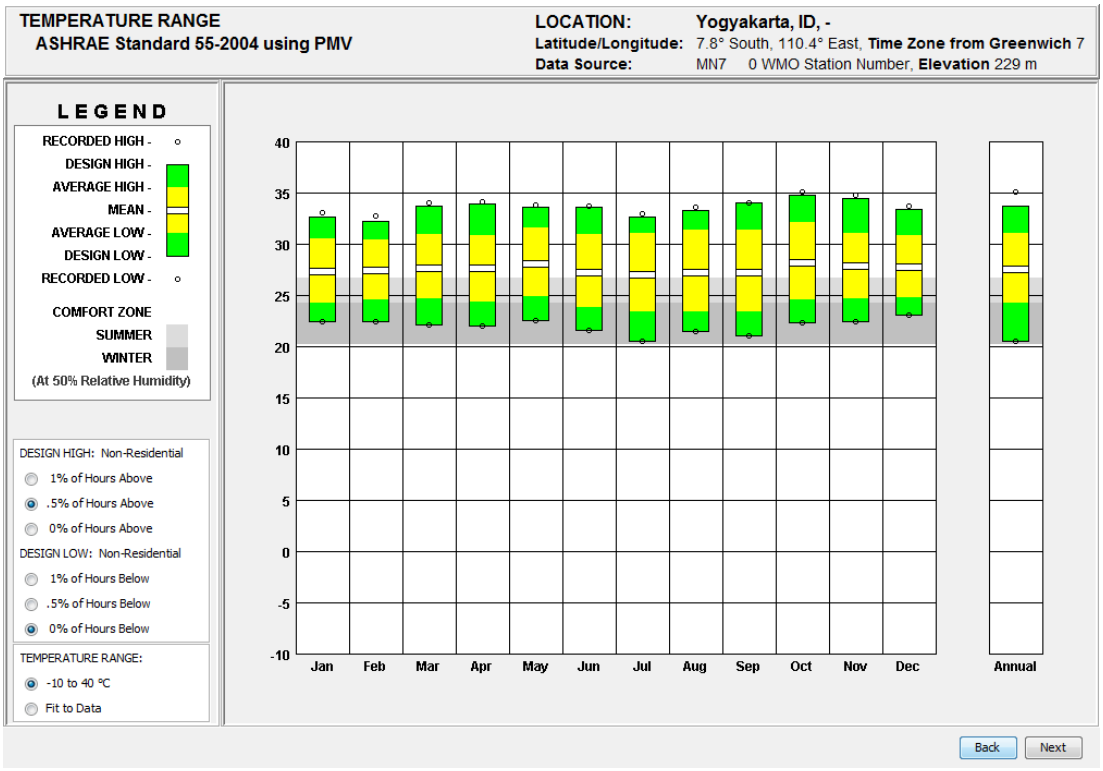
TEMPERATURE RANGE
ASHRAE Standard 55-2004 using PMV
LOCATION: Yogyakarta, ID, -
Latitude/Longitude: 7.8° South, 110.4° East, Time Zone from Greenwich 7
Data Source: MN7 0 WMO Station Number, Elevation 229 m
LEGEND
RECORDED HIGH -
DESIGN HIGH -
AVERAGE HIGH -
MEAN -
AVERAGE LOW -
DESIGN LOW -
RECORDED LOW -
COMFORT ZONE
SUMMER
WINTER
(At 50% Relative Humidity)
DESIGN HIGH: Non-Residential
1% of Hours Above
.5% of Hours Above
0% of Hours Above
DESIGN LOW: Non-Residential
1% of Hours Below
.5% of Hours Below
0% of Hours Below
TEMPERATURE RANGE:
-10 to 40 °C
Fit to Data
40
35
30
25
20
15
10
5
0
-5
-10
Jan
Feb
Mar
Apr
May
Jun
Jul
Aug
Sep
Oct
Nov
Dec
Annual
Back
Next

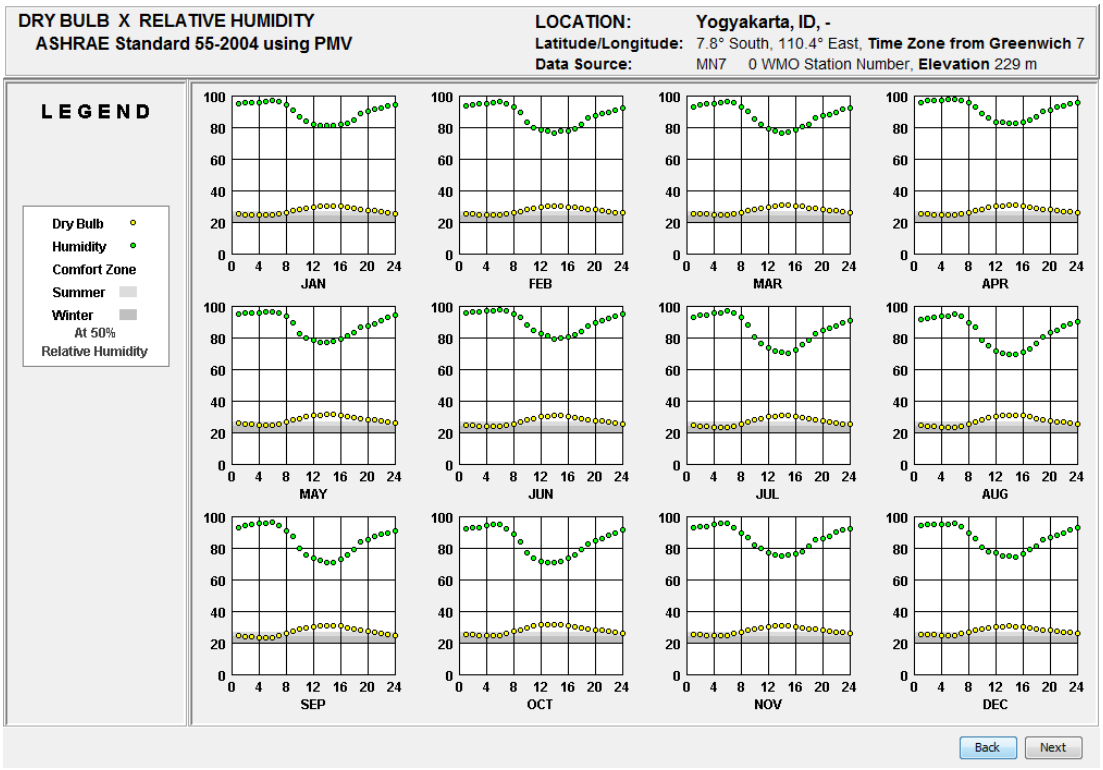
DRY BULB X RELATIVE HUMIDITY
ASHRAE Standard 55-2004 using PMV
LOCATION: Yogyakarta, ID, -
Latitude/Longitude: 7.8° South, 110.4° East, Time Zone from Greenwich 7
Data Source: MN7 0 WMO Station Number, Elevation 229 m
LEGEND
Dry Bulb
Humidity
Comfort Zone
Summer
Winter
At 50%
Relative Humidity
JAN
FEB
MAR
APR
MAY
JUN
JUL
AUG
SEP
OCT
NOV
DEC
Back
Next

Modified weather file MOWF:

WEATHER DATA SUMMARY

LOCATION: Yogyakarta, ID, -
Latitude/Longitude: 7.8° South, 110.4° East, **Time Zone from Greenwich** 7
Data Source: MN7 0 WMO Station Number, **Elevation** 229 m

MONTHLY MEANS	JAN	FEB	MAR	APR	MAY	JUN	JUL	AUG	SEP	OCT	NOV	DEC	
Global Horiz Radiation (Avg Hourly)	340	351	378	403	431	408	406	428	429	413	344	353	Wh/sq.m
Direct Normal Radiation (Avg Hourly)	203	185	214	268	383	399	324	319	290	240	178	199	Wh/sq.m
Diffuse Radiation (Avg Hourly)	196	220	223	217	181	159	200	213	221	234	217	210	Wh/sq.m
Global Horiz Radiation (Max Hourly)	1110	1046	1101	1072	954	890	885	956	1113	1057	1108	1094	Wh/sq.m
Direct Normal Radiation (Max Hourly)	990	924	1029	972	928	898	909	919	920	945	801	978	Wh/sq.m
Diffuse Radiation (Max Hourly)	488	540	537	491	428	423	442	466	520	544	532	532	Wh/sq.m
Global Horiz Radiation (Avg Daily Total)	4220	4313	4563	4765	5020	4719	4710	5039	5140	5031	4263	4404	Wh/sq.m
Direct Normal Radiation (Avg Daily Total)	2529	2279	2579	3173	4463	4616	3765	3747	3476	2934	2212	2483	Wh/sq.m
Diffuse Radiation (Avg Daily Total)	2430	2708	2695	2574	2116	1848	2328	2512	2650	2856	2685	2622	Wh/sq.m
Global Horiz Illumination (Avg Hourly)	38437	39848	42809	45447	48320	45554	45073	47475	47860	46379	39007	39985	lux
Direct Normal Illumination (Avg Hourly)	19145	15836	19314	23590	34955	36963	28552	27901	25426	21407	15411	18035	lux
Dry Bulb Temperature (Avg Monthly)	28	28	28	28	29	28	28	28	28	29	29	29	degrees C
Dew Point Temperature (Avg Monthly)	24	22	22	22	22	21	20	19	20	21	22	22	degrees C
Relative Humidity (Avg Monthly)	88	87	87	91	88	90	85	83	85	83	86	73	percent
Wind Direction (Monthly Mode)	260	270	250	250	100	60	80	180	180	160	250	290	degrees
Wind Speed (Avg Monthly)	1	1	1	1	1	1	1	2	1	1	1	1	m/s
Ground Temperature (Avg Monthly of 1 Depths)	26	26	26	26	26	26	26	26	26	26	26	26	degrees C

Back Next

TEMPERATURE RANGE
ASHRAE Standard 55-2004 using PMV

LOCATION: Yogyakarta, ID, -
Latitude/Longitude: 7.8° South, 110.4° East, **Time Zone from Greenwich** 7
Data Source: MN7 0 WMO Station Number, **Elevation** 229 m

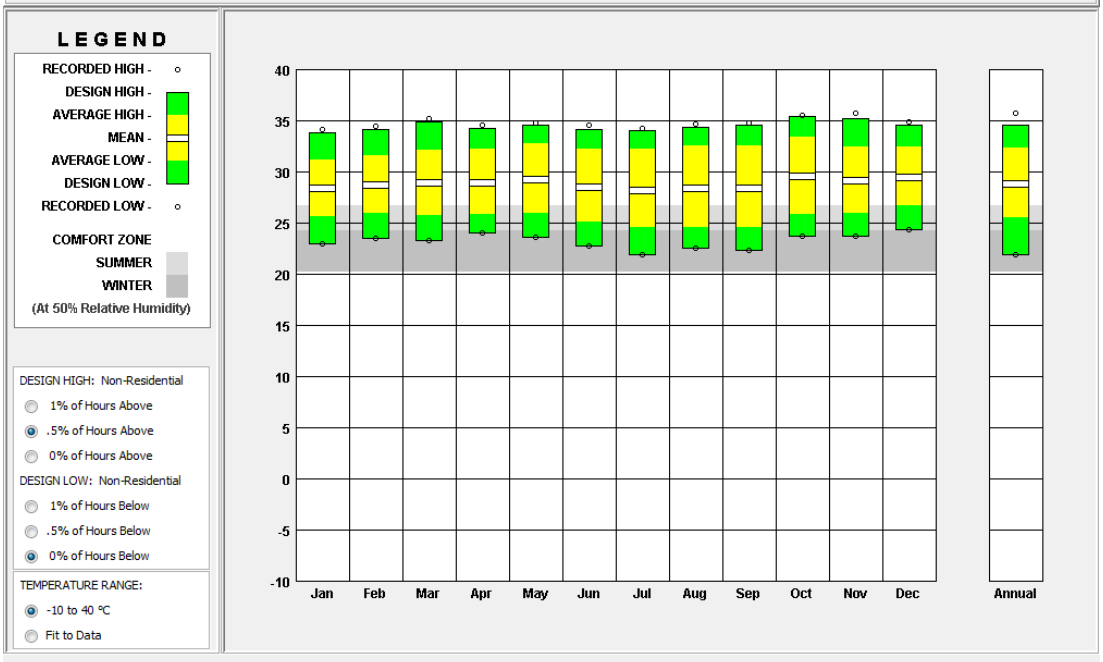

Back Next

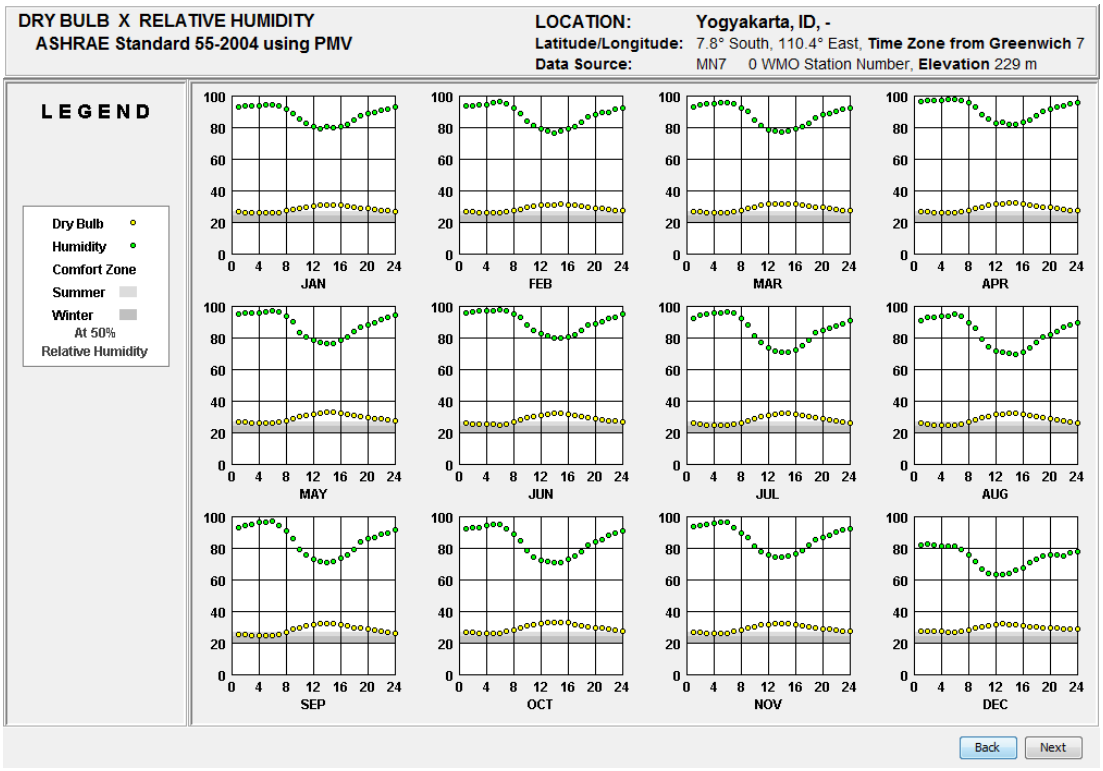
DRY BULB X RELATIVE HUMIDITY
ASHRAE Standard 55-2004 using PMV
LOCATION: Yogyakarta, ID, -
Latitude/Longitude: 7.8° South, 110.4° East, Time Zone from Greenwich 7
Data Source: MN7 0 WMO Station Number, Elevation 229 m
LEGEND
Dry Bulb
Humidity
Comfort Zone
Summer
Winter
At 50%
Relative Humidity
JAN
FEB
MAR
APR
MAY
JUN
JUL
AUG
SEP
OCT
NOV
DEC
Back
Next